Mapping Human Genetic Diversity in Asia

Article *in* Science · December 2009

DOI: 10.1126/science.1177074 · Source: PubMed

92 authors, including:

Mahmood AMEEN Abdulla
University of Malaya
304 PUBLICATIONS **4,012** CITATIONS
SEE PROFILE

Ikhlak Ahmed
Weill Cornell Medicine in Qatar
72 PUBLICATIONS **1,901** CITATIONS
SEE PROFILE

Anunchai Assawamakin
Mahidol University
86 PUBLICATIONS **915** CITATIONS
SEE PROFILE

Jong Bhak
Ulsan National Institute of Science and Technology
225 PUBLICATIONS **3,931** CITATIONS
SEE PROFILE

Supporting Online Material for

Mapping Human Genetic Diversity in Asia

The HUGO Pan-Asian SNP Consortium†

†To whom correspondence should be addressed. E-mail: ljin007@gmail.com (L.J.); liue@gis.a-star.edu.sg (E.T.L.); seielstadm@gis.a-star.edu.sg (M.S.); xushua@picb.ac.cn (S.X.)

Published 11 December 2009, *Science* **326**, 1541 (2009)
DOI: 10.1126/science.1177074

This PDF file includes:

Additional Acknowledgments

China:
The work of Shanghai group for PASNPI was supported by National Outstanding Youth Science Foundation of China (30625016, 30625019), National Science Foundation of China (30890034), Chinese High-Tech (863) Program (2006AA020706, 2006AA020704□2007AA02Z312), National Key Project for Basic Research (2002CB512900, 2004CB518605), Shanghai Leading Academic Discipline Project (B111), Science and Technology Commission of Shanghai Municipality (04DZ14003, 06XD14015, 09ZR1436400), Knowledge Innovation Program of Shanghai Institutes for Biological Sciences, Chinese Academy of Sciences (2008KIP311), and K.C.Wong Education Foundation, Hong Kong.
India:
IGIB would like to acknowledge the "Council for Scientific and Industrial Research" (CSIR), India for financial support (MLP001). It would also like to acknowledge the technical help from "The Centre for Genomic Applications" (TCGA) genotyping facility.
Indonesia:
This study was supported as part of the Eijkman Institute program on Indonesian Human Genome Diversity in Biotechnology (Principal Investigator - Herawati Sudoyo), with funding managed through the Indonesian Ministry for Research and Technology. We thank Dr. Yahwardiah Siregar and Prof. Gontar Siregar (University of North Sumatra, Medan), Prof. Dasril Daud and Prof. Irawan Yusuf (Hasanudin University, Makassar), Dr. Marten Caley and Dr. Matius Kitu (Heads of District Health Agencies, Sumba), and Dr. Paul Sukarno Manoempil and Dr. Eduardus Kleruk (Head of District Health Agencies, Alor and Flores), and their respective field teams for their support and participation in the field work with the ethnic populations of Tanah Batak, South Sulawesi, Sumba, Alor and Flores, respectively.
Japan:
This work was in part supported by Grant-in-Aid for Scientific Research on Priority Areas "Comprehensive Genomics" and "Genome Medicine" from the Ministry of Education, Culture, Sports, Science and Technology of Japan.
Korea:
The work of KNIH group was supported by intramural grants from the Korea National Institute of Health(KNIH), Korea Center for Disease Control and Prevention, Republic of Korea (Project No.: 2910-213-207).
The work of KOBIC group was supported by a grant from "KRIBB Research Initiative Program", MIC(Ministry of Information and Communication), Korea, under the KADO (Korea Agency Digital Opportunity & Promotion) support program, and MOST international collaboration fund (K20724000003-07B0400-00310). We also thank Jung Sun Park, So Hyun Hwang, Daeui Park, Yongseok Lee, Seongwoo Hwang and Maryana Bhak.
Much of the calculation for this work was carried out by computer clusters provided by KOBIC, KRIBB, Korea.
Malaysia:
Juli Edo for anthropological expertise and liaison with Jabatan Hal Ehwal Orang Asli (JHEOA).
Ministry of Science, Technology and Innovation (MOSTI), Malaysia for IRPA grant # 36-02-03-6006
1) This study was supported by The Fundamental Research Grant Scheme (FRGS Top-Down), Ministry of Higher Education, Malaysia. Grant number: 203/PPSP/6170025.
2) We would like to acknowledge our appreciation for the contribution from colleagues from the School of Medical Sciences, School of Health Sciences and School of Dental Sciences, Universiti Sains Malaysia. .
The Philippines:
People:

the Aetas, Agtas, Atis, Mangyan-Irayas, Mamanwas, Manobos for providing us the samples;
Miriam M. Dalet, DNA Analysis Laboratory, Natural Sciences Research Institute, University of the Philippines;
Minerva S. Sagum, DNA Analysis Laboratory, Natural Sciences Research Institute, University of the Philippines;
Dr. Saturnina C. Halos, DNA Analysis Laboratory, Natural Sciences Research Institute, University of the Philippines;
Dr. Victor J. Paz, Archaeological Studies Program, University of the Philippines, Diliman and Dr. Sabino G. Padilla, Department of Behavioral Sciences, University of the Manila.
Agencies:
Agusan del Sur Provincial Government, Christ Faith Fellowship Church Mission, Surigao del Norte, Dao Bible Believing Church, Mangyan Tribal Church Association (MCTA), National Commission on Indigenous Peoples (NCIP), Office of the Mayor, Malay of the Province of Aklan, Philippine National Red Cross (PNRC), Subic Bay Metropolitan Authority (SBMA) Ecology Center, Surigao del Norte Provincial Government

Singapore:
This research was supported by the Agency for Science Technology and Research (ASTAR). The Genome Institute of Singapore also wishes to acknowledge the organizational assistance of Chaylan Long.

Taiwan:
This research project was supported by grants from the National Science and Technology Program for Genomic Medicine, National Science Council, Taiwan (National Clinical Core for Genomic Medicine NSC95-3112-B-001-010 and National Genotyping Center NSC95-3112-B-001-011), and the Academia Sinica Genomic Medicine Multicenter Study.

Thailand:
1. The staff of the Tribal Research Institute, Chiang Mai, Thailand, for field work organization.
2. This research project was supported by the Thailand Research Fund, Grant Numbers PHD/0011/2544, BGJ/26/2544, PHD/0058/2545, BGJ4580022.
3. Sissades Tongsima and the team from biostatistics and bioinformatics laboratory acknowledge the Thailand Research Fund and the Thailand Research Fund and the National Center for Genetic Engineering and Biotechnology for supporting this work.

USA:
We would like to acknowledge Shoba Gopalan for technical support and Michele Cargill for helpful comments and suggestions.

CONTENTS

Supplementary Figures

1. METHODS

1.1. Populations, Samples & Genotyping

DNA samples from 1,903 unrelated individuals representing 71 populations from China, India, Indonesia, Japan, Malaysia, the Philippines, Singapore, South Korea, Taiwan, and Thailand were collected and genotyped. Additionally, genotypes for 60 unrelated European-Americans (CEU, Utah residents with ancestry from northern and western Europe), 60 Yoruba (YRI, Yoruba from Ibadan, Nigeria), 45 Chinese (CHB, Han Chinese in Beijing), and 44 Japanese (JPT, Japanese in Tokyo) were downloaded from the International HapMap Project Website (S*1*). All samples were collected with informed consent and approved by local ethics and institutional review boards (IRBs) in the respective countries. Copies of IRB approvals were reviewed and deposited with the Policy Review Board (PRB) of the Pan Asia SNP Consortium. Prior to genotyping and analysis, all samples were stripped of personal identifiers (if any existed). The 75 populations represent 10 language families. Detailed sample information is shown in **Figure 1**, **Figure S31,** and **Figure S32**.

Genotyping with the Affymetrix Genechip Human Mapping 50K Xba array was performed at eight different genotyping centers (**Table S2**), according to the manufacturer's protocols (Affymetrix, *GeneChip Mapping 100K Assay Manual rev. 3*, 2004). .CEL files containing raw intensity data were centralized and analyzed at the Genome Institute of Singapore. The files were analyzed first with the DM algorithm using the Affymetrix Genechip Data Analysis Software (GDAS). Samples with a call-rate below 90% (N=142) were excluded from further analyses. Files passing this QC filter were next analyzed in three separate runs of the Affymetrix BRLMM algorithm. Again, samples with a call-rate below 90% (N=20) were excluded from further analysis. In addition, 22 sample duplicates were discovered, and the member of each pair with the lower call-rate was dropped from downstream analyses. Of the 1,903 DNA samples attempted, 1,719 (90%) provided data that passed our QC filters. Sample

call-rates ranged from 90.28-99.96% with a mean of 98.81% and median of 99.49%.

We also applied SNP filtering as described in **Table S4**. A total of 4,166 SNPs (7%) were removed from downstream analyses, resulting in a final dataset containing genotypes for 54,794 autosomal SNPs. The SNPs are fairly evenly spaced across all of the autosomes, with 1,189 SNPs mapping to the X chromosome.

1.2. Data integration

We integrated three data sets [HapMap data (S*2*), PanAsia 50K data, and HGDP-CEPH 650K data (S*3*)] according to SNP ID (rs number). This effort yielded 19,934 SNPs genotyped in all 126 population samples (S*4*). By comparing the genotypes of five Melanesian samples (AX-ME) that had been typed in both the PASNPI and HGDP-CEPH 650K data sets, only 80 genotypes were discordant in the two datasets, resulting in genotyping concordance between Affymetrix and Illumina technologies of greater than 99.9% (S*4*). The physical positions of SNPs and the coding of alleles were synchronized to the forward strand on *Homo sapiens* Genome Build 36. The average spacing between adjacent markers is 137.7 kb, with a minimum of 17 bp and a maximum of 29.6 Mb, the median inter-marker distance (IMD) is 65.4 kb.

1.3. Determination of Ancestral alleles

The ancestral states of 42,793 SNPs were determined by genotyping 21 chimpanzees and 1 gorilla. All SNPs called homozygous in chimps and gorilla were used to assign the ancestral state as previously described (S*5, 6*)

1.4. AMOVA analysis

The genetic structure of populations was investigated here by an analysis of molecular variance (AMOVA) as implemented in Arlequin 3.0 (S*7*). We defined various groupings of populations to be tested in this way (see **Table S1** for results and details

of the design). A hierarchical analysis of variance partitions the total variance into covariance components due to intra-individual differences, inter-individual differences, and/or inter-population differences. The covariance components are used to compute fixation indices, as originally defined by Wright (S*8*), in terms of inbreeding coefficients, or, later, in terms of coalescent times by Slatkin (S*9*). AMOVA was performed by Arleguin 3.0 with 100,000 permutations. The population groupings and results are shown in **Table S1** where the confidence intervals are based on 100,000 bootstrap replicates across loci.

Consistent with previous results, the average proportion of genetic variation among individuals from different populations only slightly exceeds that among individuals from within a single population. The within-population component of genetic variation was estimated at 95 - 96%, as shown in **Table S1**, when only 72 Asian populations were considered. When including the non-Asian populations, this within-population component of genetic variation drops to 93 - 94%.

1.5. Genetic distance for individuals

We used an allele sharing distance (S*10, 11*) as a measure of genetic distance between individuals and a 1928 × 1928 inter-individual genetic distance matrix was generated from genotypes of 54,794 autosomal SNPs.

1.6. Principal component analysis for individuals

Principal components analysis (PCA) was performed at the individual level using EIGENSOFT version 2.0 (S*12*).

1.7. Genetic distance for populations

Three genetic distance measurements, F_{ST} (S*13*), Nei's standard distance (S*14*), and Nei's D_A (S*15*) were used to estimate genetic divergence among populations.

1.8. Tree reconstruction

Distance based individual and population trees were reconstructed using the Neighbor-Joining algorithm (S*16*) with the Molecular Evolutionary Genetics Analysis software package (MEGA version 4.0) (S*17*). Maximum likelihood trees of populations were reconstructed using maximum likelihood method (S*18*) with CONTML program in PHYLIP package (S*19*).

1.9. Great circle distance

Great circle distance calculations followed the approach of Ramachandran et al. (S*20*), Rosenberg et al. (S*21*) and Jakobsson et al. (S*22*). For world-wide populations, Addis Ababa (9° N, 38° E) was used as starting point in East Africa. Waypoint routes followed Ramachandran et al. (S*20*). Paths involving Africa (including the Mozabite population) passed through Cairo, Egypt (30° N, 31° E); paths involving Europe (excluding Adygei), the Middle East (excluding Mozabites), Asia and Oceania passed through Istanbul, Turkey (41° N, 28° E); paths involving Oceania passed through Phnom Penh, Cambodia (11° N, 104° E); paths involving the Americas all passed through Anadyr, Russia (64° N, 177° E) and Prince Rupert, Cannda (54° N, 130° W). For populations within Asia, no waypoint was used.

1.10. Partial and multiple Mantel tests

1.10.1. Tests for pre-historical divergence and isolation by distance effects

We used partial and multiple Mantel tests to simultaneously test pre-historical divergence effects and isolation by distance (IBD) effects. The general idea is that the IBD process occurs on a much smaller time-scale than long-term historical isolation or deep-time coalescence (S*23*). Therefore, the obvious and simpler solution would be to apply Mantel tests correlating genetic and geographic distances for each clade (or cluster, or group) separately. There are three different matrices to be analyzed: 1) genetic distances; 2) geographic distances, and 3) a model matrix expressing

pre-historical divergence (S*23*). Logarithm transformed F_{ST} (S*13*) values were used as genetic distances and great circle distances (S*20*) were used as geographic distances. If groups of local populations could be explicitly defined to diverge under long-term historical processes, multiple Mantel tests could be used to partition the contemporary (IBD) and historical effects. Pre-historical divergence can be inferred by "external" information (biogeographical and ecological data) or can be derived from phylogenetic analysis (S*23*) (see also Santos et al. (S*24*), for a recent example). The groups of populations belonging to the same clade, or group, could be linked in a pairwise model matrix (S*25-28*), in which the value 1.0 indicates that two populations are "linked" (within the same group), and zero elsewhere (S*23*). In our case, populations were grouped according to PCA results (**Fig. 2**) and STRUCTURE (**Fig. 1**, **Fig. S1-S13**) & *frappe* results (**Fig. S14-S26**).

The other approach is to use Mantel tests under a multiple correlation and regression design (S*29-31*) to simultaneously evaluate the effect of long-term historical divergence and effect of more recent and local IBD. In this case, it would be possible to establish which part of the total explained variance of genetic distances could be attributed to these effects and to the overlap between them. These relative values could be obtained simply by performing Mantel tests, using each effect separately and combined into a single model, as described below.

Using the notation by Legendre and Legendre (S*31*) and following Telles et al. (S*23*), the unexplained variation in genetic divergence (d) is given by 1 - R^2_T, where R^2_T is the squared correlation coefficient of a Mantel test performed using a general linear model that includes both matrices (geographic distances, to evaluate IBD, and the binary model matrix representing long-term historical divergence), which corresponds to the portion (a + b + c). The overlap between IBD and long-term historical divergence (b) is equal to (a + b) + (b + c) - (a + b + c), where (a + b) is given by the R^2 of the Mantel test using geographic distances only (R^2_I), and (b + c) is given by the R^2 of the Mantel test using model matrix (R^2_H). We can then partition variation explained by IBD only (a) and the long-term historical divergence only (c), simply by (R^2_I - b) and (R^2_H - b), respectively.

1.10.2. Tests for the correlation of linguistic and genetic affinity

The Mantel test designs were similar to that above. Pairwise F_{ST} values were used as genetic distances between populations and great circle distances were used as geographic distances. Linguistic affinities between populations were coded by a binary model matrix, in which the value 1.0 indicates that two populations are belonging to the same linguistic family, and zero elsewhere.

1.11. Simulation of genotypic data under isolation by distance (IBD)

To further investigate whether the genetic structure observed in this study reflects pre-historical migration signals or resulted from isolation by distance effects, we carried out a simulation study under isolation by distance using the computer program IBDsim (S*32*) version 1.0. We employed a lattice model without edge effects so that habitats of sub-populations have complete homogeneity in space, sub-populations were assumed to split simultaneously without hierarchical structure and without directional migrations. Dispersal was constant in time, and throughout the simulation, migration rates were set as a function of geographical distance. 100 populations were simulated, phylogenetic trees were reconstructed, and heterozygosity was calculated for each population and group of populations from the simulated data.

We also performed forward time simulations of isolation by distance effects under the same assumptions described above. The allele frequency spectrum of the MRCA is derived from the autosomes of 60 unrelated YRI samples from the HapMap project. Both one-dimensional and two-dimensional IBD were simulated.

1.12. Structure analysis

1.12.1. Full data set for *structure* analysis

The program STRUCTURE implements a model-based clustering method for inferring population structure using genotype data (S*33*). We performed STRUCTURE

analysis for the full dataset consisting of 1,928 individuals and 54,794 autosomal SNPs. We ran STRUCTURE for the full data set from *K* = 2 to *K* = 20, and repeated it 3 times for each single *K*. All structure runs performed 20,000 iterations after a burn-in of 30,000, under the admixture model, and assumed that allele frequencies were correlated (S*33*).

1.12.2. Random sampling of markers for STRUCTURE analysis

In Version 2.1, the STRUCTURE program implemented a model that allows for "admixture linkage disequilibrium" in which correlations that arise among linked markers are modeled as the result of admixture (S*34*). However, the program was not designed to model the linkage disequilibrium (LD) that occurs within populations between tightly linked markers (so called "background LD") (S*33, 34*). In our data, 10% of the SNPs on the XBA array have inter-marker distances (IMD) <0.2 kb; 52% of SNPs have IMD < 20kb; and 95.6% of SNPs have IMD <200 kb. Previous studies have shown that in many non-African populations, the extent of linkage disequilibrium can range up to 100 kb or sometimes more(S*2, 35-38*). Therefore, we chose subsets of randomly sampled markers with IMD larger than 500 kb to avoid strong LD within populations. Due to the computational intensity of STRUCTURE analyses, we used 10 sub-datasets (S1~S2) with IMD larger than 500 kb, each dataset containing approximately 4,300 SNPs, distributed across the 22 autosomes.

1.12.3. STRUCTURE settings

All STRUCTURE runs used 20,000 iterations after a burn-in of length 30,000, with the admixture model and assuming that allele frequencies were correlated (S*33*). To evaluate whether this burn-in time was sufficient for convergence, we performed longer runs for dataset S1, all with a burn-in period of 100,000, and we compared results based on later iterations with those of the first 20,000 iterations after the burn-in. For each of *K*=2 ~ *K*=20, three runs were performed using dataset S1 and the correlated allele frequencies model. Estimates of membership coefficients were

separately obtained using the first 20,000 iterations after completion of the burn-in, iterations 40,001~60,000 after burn-in, iterations 60,001~80,000, and iterations 80,001~100,000. Using a symmetric similarity coefficient (S*39*), each of these four stages in each run was compared to each stage in the other two runs with the same value of *K*, as well as to the other three stages from the same run. In all cases of $K < 8$, similarity scores were 0.98 or greater. For larger *K*s (> 7), the splitting order of the clusters varied slightly across runs involving different sub-data sets, as we show in the following section. However, the membership coefficient estimates were still highly similar (> 0.85) for the four stages, indicating that membership coefficient estimates were nearly identical both for different runs with the same *K* as well as for the four stages of the same run (S*21*). In addition, we found there were no changes in the splitting order of the clusters in the four stages of the same run. Therefore, the estimates would not be substantially different if longer iterations were used.

We also checked the distribution of alpha, as suggested by the authors of the structure program. After 20,000 iterations, where it became relatively constant indicating convergence. To ensure that the burn-in length was adequate, we performed all STRUCTURE runs with a burn-in length of 30,000. We ran STRUCTURE from K = 2 to K = 20, and repeated it 10 times for each single *K*. Finally, for each sub-dataset, we ran STRUCTURE from *K* = 2 to *K* = 20, and repeated it 10 times for each single *K*: we submitted a total of 10 × 10 × 19 = 1,900 jobs for STRUCTURE analysis.

1.12.4. Analysis of STRUCTURE results: Similarity coefficients and Determination of primary clusters

As recommended by the authors of STRUCTURE, one strategy for analyzing highly structured data such as ours is to run multiple values of *K* (the number of clusters) and to select the *K* that maximizes the posterior probability of the data (S*33, 40*).

However, for very complex datasets that include many groups, this criterion is difficult to apply: the algorithm may converge to numerous distinct clustering schemes for a given value of *K*, so that estimated probabilities differ across runs (S*41*). For the full dataset, the maximum posterior probabilities of repeat runs were observed to increase consistently while *K* was less than 16. For the ten data sets (S1-S10), the maximal posterior probabilities of repeat runs were also seen to increase with increasing *K*. We carefully compared the membership plots of (1) different *K*s of the same data set, (2) between different data sets, and (3) between subset of data and full data set (see **Figure S1 ~ S13**). The symmetric similarity coefficient (SSC)(S*39*) was computed as a measure of the similarity of the outcomes of the two population structure estimates. For a given *K*, both SSC of each pair of runs within the same data set and each pair of runs between data sets were calculated using the Greedy algorithm of CLUMPP (S*39*). In all cases of $K < 8$, similarity scores were 0.98 or greater; for larger *K*s ($K > 7$), the splitting orders of clusters varied across different runs and different data sets. However, for the same cluster mode, the membership coefficient estimates were still high (> 0.85).

The primary clusters we identified from both the full data set and sub-datasets show little variation among individuals of the same population, and correspond overwhelmingly to language families or ethnic groups: (1) The ***Altaic*** cluster is comprised mainly of Altaic and Sino-Tibetan speaking populations; (2) The ***Tai-Kadai/Sino-Tibetan*** cluster includes mainly Tai-Kadai and Sino-Tibetan speaking populations; (3) The ***Hmong-Mien*** cluster is seen exclusively in Hmong-Mien speaking populations; (4) The ***Austro-Asiatic*** cluster delineates mainly Austro-Asiatic speaking populations; (5) The ***Negrito-W*** cluster characterizes the two Malaysian Negrito populations; (6) The ***Negrito-E*** cluster is found mainly among Philippine Negrito populations; (7) The ***Papuan*** cluster characterizes mainly Papuan and East Indonesian populations; (8) The ***Austronesian*** cluster is associated mainly with Austronesian speaking populations; (9) The ***Dravidian*** cluster defines mainly Indo-European and Dravidian speaking Indian populations; (10) The ***Indo-European***

cluster defines mainly Indo-European speaking populations; the other four clusters correspond to single populations, i.e. the Bidayuh population of Malaysia, the proto-Malay Temuan population, the Mlabri) inhabiting Thailand, and the African cluster confined mainly to the YRI.

We found that when $K > 14$ in sub-datasets or $K > 15$ in the full dataset, the newly emerging clusters were generally confined to single populations, but that the splitting order varied greatly for larger K's across different runs and different data sets. Considering the biological meaning of the clusters and the purpose of our study (we focus on general, continent-wide patterns in this initial study), we used $K \leq 14$ to analyze population structure in the worldwide samples and in further analysis.

1.12.5. Constructing a phylogenetic tree of STRUCTURE clusters

Although the STRUCTURE analysis was designed to identify distinct and putatively ancestral components without incorporating population-affiliations for each individual, it does not reveal the relationships among such components. However, the phylogenetic relationships of these clusters (referred to as the "component tree"), given their statistical independence, should reveal an evolutionary history that is less perturbed by recent gene flow and admixture than is a population phylogeny. Therefore, we reconstructed a phylogenetic tree relating the clusters based on allele frequencies in each cluster inferred from the STRUCTURE analysis (K=14). The overall pattern of this component tree is similar to that of the population tree (**Fig. 1**) with a few revealing exceptions. The component we associate with Austronesian speakers now groups with the mainland East Asian components, consistent with the idea that this language family expanded from mainland East Asia – possibly following the development of rice agriculture, as has been previously hypothesized on archeological and linguistic grounds (S*42*). The Negrito and Papuan groups are now closer to the root of the East Asian and Southeast Asian clades, with the European and Indian groups positioned outside the clade. This suggests that the divergence of the Negrito groups and the other Asian populations occurred after the divergence of

Asian and European populations.

1.13. *frappe* analysis

The program *frappe (S43)* implements a maximum likelihood method to infer the genetic ancestry of each individual. As in STRUCTURE analysis, this method considers each person's genome as having originated from *K* ancestral, but unobserved, populations whose contributions are described by *K* coefficients that sum to 1 for each individual (S*3*). We performed *frappe* analysis on the same set of 1,928 individuals and 54,794 SNPs, and two subsets of the full data (S1, S2). The program was run for 10,000 iterations from *K*=2 to 14. The results are shown in **Figure S14 ~ S26**. The results from *frappe* analysis showed a general concordance with that of STRUCTURE. The symmetric similarity coefficient (SSC)(S*39*) was computed as a measure of the similarity of the outcomes of the two population structure estimates. In all cases of $K < 9$, similarity scores between *frappe* results and STRUCTURE results were 0.93 or greater; for larger *K*s ($K > 8$), the splitting orders of clusters varied between *frappe* and STRUCTURE. However, for the same cluster mode, the membership coefficient estimates were still high (> 0.70). Notably, those main clusters that we identified in STRUCTURE analysis were all identified by *frappe* as well.

1.14. Forward time simulation

1.14.1. Modeling one-wave and two-wave hypothesis

By considering various models for the peopling of Asia, we posited three potential models, as illustrated in **Figure S29**. In Model 1, the ancestors of Asians (AS) and Europeans (EU) separated from the ancestors of Africans (AF) and Negritos (NG) 100 thousand years (5,000 generations) ago, AF and NG separated from their MRCA 3,000 generations ago, and AS and EU separated from their MRCA 2,000 generations ago. In Model 2, NG has an MRCA with AS and EU after separating from AF 5,000 generations ago, but NG separated from the MRCA of AS and EU 3,000 generations

ago, and then AS and EU separated 2,000 generations ago. In Model 3, NG has an MRCA with AS and EU after separation from AF 5,000 generations ago, but EU separated 3,000 generations ago before the separation of NG and AS 1,000 generations later. Models 1 and Model 2 are both consistent with a two-wave hypothesis, while Model 3 suggests a “one-wave” hypothesis.

The effective population sizes of the four populations are assumed to be constant following population subdivision at: 10,000, 1,000, 5,000, and 5,000 for Africans (AF), Negritos (NG), Asians (AS), and Europeans (EU), respectively. For all three models, a bottleneck size of 100 chromosomes is assumed for NG, a bottleneck size of 400 chromosomes is assumed for both AS and EU. Gene flow proportions from AS to NG were set to different levels (M=0.005 ~ 0.95) to examine at which level the topology of trees would change.

The allele frequency spectrum of the MRCA is derived from the autosomes of 60 unrelated YRI samples from the HapMap project. 10,000 SNPs were simulated, and 100 chromosomes were sampled for each population at the end of the simulations.

1.14.2. Computer simulation exploring the possibility of an undetected two-wave signal

Although the observed genetic relationships of modern Asian populations did not support a two-wave hypothesis, there is still a formal possibility that strong gene flow from other Asian populations into the Negrito populations contributed to the observed pattern of the trees. To test this hypothesis, and to examine how much gene flow from other Asian populations (AS) would be required to alter the topology in a way that is consistent with Models 1 or 2, we applied forward time simulations according to the assumptions outlined above.

Results from these simulations are shown in **Figure S30**. For model 1, when the gene flow proportion (M) is greater than 0.02, bootstrap values start to decrease,

however, the topology of the tree remains unchanged. The topology of the tree changes when M ≥ 0.15, however, NG still remains outside the clade of AS and EU, even at extremely high values of M = 0.95. For model 2, the topology of the tree is unchanged until M ≥ 0.45, when NG and AS cluster together, however the bootstrap value is very low (51%). As the gene flow proportion (M) increases, bootstrap values increase, reaching 100% when M ≥ 0.80.

Our simulation results indicate that model 1 is not compatible with the empirical data, and model 2 is only compatible if gene flow from other Asian populations to the Negritos has been fairly extreme, with more than 50% of Negrito chromosomes coming from other Asian populations, without dramatically affecting the Negrito phenotype.

1.15. Haplotype-based analyses

1.15.1. Haplotype estimation

Haplotypes of 22 autosomes were estimated for each individual from its genotypes with fastPHASE (S*44*) version 1.2. “Population labels” were applied during the model fitting procedure to enhance accuracy. The number of haplotype clusters was set to 30, the number of random starts of the EM algorithm (-T) was set to 20, and the number of iterations of EM algorithm (-C) was set to 50. This analysis was used to generate a “best guess” estimate of the true underlying patterns of haplotype structure (S*44*). We ran fastPHASE for PanAsia data set (54,794 SNPs shared by 75 populations) and combined PanAsia-HGDP data set (19,934 SNPs shared by 126 populations, see **1.1** and **1.2**) separately. For both data sets, only unrelated individuals were included.

1.15.2. Haplotype diversity

Heterozygosity for single SNPs (HS_e) was calculated based on SNP allele frequencies. To calculate heterozygosity for haplotypes (HH_e), the genome was divided into 5 ~ 500 kb bins, with each distance bin having at least 2 SNPs per 5 kb

(bins not satisfy this criterion were not included in the following calculation), frequencies of haplotypes were counted and HH_e were calculated for each region based on haplotype frequencies. Considering the substantial variation in recombination rate across human genome (S*2, 45*), we adopted a sliding window strategy and allowed the window to slide by half its length each time. For example, two adjacent 100 kb windows could overlap by 50 kb. For each population, HH_e was averaged over all windows.

1.15.3. Haplotype sharing analyses

To investigate population or group relationships at the haplotype level, we estimate haplotypes shared between populations or groups considering both (a) type only and (b) type with frequency. In the analysis of (a), we compared the average number of haplotypes across these sliding-window regions in each population or group. In the analysis of (b), the frequency of haplotype was also considered. All the analyses were also extended to the comparisons of three or more populations or groups.

1.15.3.1. Haplotype sharing by type

In this analysis, we considered consecutive sets of markers within each bin as defined above, and counted the total number of haplotypes observed across regions. We asked how many haplotypes were, on average, shared by two populations / groups. Since the results could be affected by varying sample size among populations, we sampled 200 chromosomes without replacement in each population when counting the number of haplotypes in each genomic interval. The sampling procedure was repeated 100 times and the results were averaged for each genomic interval.

1.15.3.2. Haplotype sharing by both type and frequency

Haplotype sharing (*HS*) between populations or groups was estimated as the proportion of sharing haplotypes in between populations or groups (S*46*). Suppose we

have two populations, A and B, the total number of haplotypes is n_A and n_B for population A and population B respectively, we denote each haplotype in population A that can be also found in population B as HA_i, its frequency is denoted by fA_i; in the same way, each haplotype in population B that can be also found in population A and its frequency are denoted by HB_j and fB_j respectively. Haplotype sharing between population A and B (HS_{AB}) was defined as:

$$HS_{AB} = \frac{\sum_{i=1} HA_i \, fA_i + \sum_{j=1} HB_j \, fB_j}{n_A + n_B}$$

The asymmetric *HS* can be also estimated accordingly, i.e. the proportion of haplotypes in population A that can be also found in population B (HS_A) was defined as:

$$HS_A = \frac{\sum_{i=1} HA_i \, fA_i}{n_A}$$

The proportion of haplotypes in population B that can be also found in population A (HS_B) was defined as:

$$HS_B = \frac{\sum_{i=1} HB_i \, fB_i}{n_B}$$

Considering the substantial variation of recombination across human genome (S*2, 45*), we adopted a slide window strategy and *HS* was calculated in each window (5-kb ~ 500-kb bin) for population/group pairs. The adjacent sliding windows were overlapped by half of the window, i.e. the sliding windows moves forward half of distance bin each time.

Since the results could be affected by various sample size among populations, we sampled 200 chromosomes (equal to the chromosome size of 100 individuals) with

replacement in each population/group when counting the number of haplotypes in each genomic interval. The sampling procedure was repeated 100 times and the results were averaged for each genomic interval.

1.15.3.3. Identification of population/group private haplotypes

Considering the possibility of gene flow among human populations, historical inferences from haplotype sharing analyses could be affected by either ancient or recent admixture. We identified population/group private haplotypes by comparing multiple populations/groups which are interested in inferences. For example, in this study, since we are interested in the pre-historical relationship among East-Asian (EA), Southeast Asian (SE) and Central-South Asian (CSA) populations, we defined a haplotype found only in EA sample but not observed in either SE or CSA samples as an EA private haplotype, the same criterion was applied to identify private haplotypes in SE and CSA samples as well. In subsequent comparisons, as in the above analyses, type only or type with frequency were considered separately, the framework of sampling was the same as described above.

1.15.3.4. Reconstructing phylogenetic trees of populations/groups with population/group private haplotypes

Population/group private haplotypes were used to reconstruct phylogenetic relationship of populations/groups. Pairwise distances between haplotypes were calculated and summarized for all comparisons, a distance matrix was created among populations/groups in each sliding window, and a neighbor-joining tree (S*16*) based on these distance matrices was constructed.

2. Supplementary description and discussions

2.1. Additional notes on genotyping and integration of data from multiple centers

As we mentioned in Methods, genotyping with the Affymetrix Genechip Human Mapping 50K Xba array was performed at eight different genotyping centers (**Table S2**). We were concerned about introducing a systematic bias in the data due to differences amongst the genotyping centers, and therefore implemented several measures to insure uniformity among the sites. First, all sites underwent training on the Affymetrix 50K platform and this was conducted by the same technical support manager for every site. Each site was required to pass the training with a set of control samples. Secondly, a call rate cut-off of 90% was used for inclusion of samples into the study. Samples falling below this cut-off were excluded from the study. A total of 162 samples were excluded based on this criterion. The resulting mean call rates for each of the 7 sites was very high with surprisingly very little variation, ranging from 96.2% to 99.2% across sites. Furthermore, some of the genotyping centers served as host sites for more than one country (and site of DNA collection), increasing our confidence that geographic bias was not confounding the technical implementation of the study. For example, the Genome Institute of Singapore (GIS) hosted the genotyping of samples collected in Malaysia, the Philippines (including all Negrito populations from both countries), Thailand and Indonesia, in addition to its own collection of samples from Singapore. Lastly, some of the populations were composed of samples collected and run by more than one genotyping center. For example, samples of Han Chinese were run by three different centers; Malay and Japanese, as well as two independently collected samples of the Miao population were each run at two different genotyping centers. Based on the high call rates and the minimal variation across sites, coupled with some of the sites running a variety of geographic samples with little or no discernible variation, we feel confident that conclusions formed from the data reported here represent geographic and population inferences

rather than technical effects. Finally, we observed very high concordance for 5 AX-ME samples that were genotyping both in out study as well as the HGDP-CEPH 650K dataset.

2.2. Additional notes on the population samples and related issues

We focused our attention on the initial peopling of East and Southeast Asia, and the most population samples were collected from Southeast Asia, with less emphasis on South and Central Asia, and few samples from elsewhere in Asia. A consensus has developed that Southeast Asia was the site of initial entry of modern humans on the basis of archeological and genetic data. Thus testing a comprehensive collection of Southeast Asia populations is necessary to delineate the process in more detail. Since Southeast Asia harbors the greatest linguistic and ethnic diversity in the continent, we felt it important to "over" sample populations from Southeast Asia. While Central Asian populations are represented only by the Uyghur, we included the CEPH-HGDP samples in the combined dataset. In addition, our sampling from northern East Asia (including multiple samples of Han Chinese from Beijing, Shanghai, Guangzhou, and very recent immigrant communities in Taiwan and Singapore; Koreans; Japanese; and Ryukyuans) is respectable, particularly since linguistic diversity is much less in north Asia than Southeast Asia, and again, we included the CEPH-HGDP samples in the combined dataset. The Ainu, which we were unable to sample, are often thought to represent the descendants of an early migration to East Asia, but Y chromosome data suggests that the Ryukyuans (who are included in our sampling) share substantial connections with the Ainu (S*47*).

2.3. Additional notes on STRUCTURE analyses

We observed that the STRUCTURE results from the full dataset producesd inferences that differ from those based on the subsets in larger Ks (**Fig. S8 ~ S13**). We noticed that the difference between the full dataset and subsets is in the proportion of admixture levels (or membership coefficients) of individuals, the other differences

were due to the different splitting order of clusters, but the cluster modes are consistent. The background admixture present in the results of the full dataset could result from the LD between closely linked markers, because the program STRUCTURE assumes the loci are in linkage equilibrium within populations. The program cannot handle markers that are extremely close together. Even in the latest version, which implemented a "linkage model", STRUCTURE can only deal with weakly linked markers. Because, (1) in our data, there are 10% SNPs with between marker distance (BMD) <0.2 kb, 52% of SNPs with BMD < 20 kb, 95.6% of SNPs with BMD <200 kb; (2) although closely linked SNPs are not necessarily in strong LD, on average, strong LD in Asian and European populations can extend to 100 kb or more (*S2, 35-38*). Therefore, we did not think it is fully appropriate to perform STRUCTURE analysis using the full dataset, so we also used reduced datasets to avoid LD (see Methods for details). However, we found the STRUCTURE performed better than expected under the situation of LD (as the case of full dataset). Because all the cluster modes present in dataset S1 were observed frequently in the other datasets or in the full dataset, and it reflects the full picture of the cluster modes in PanAsia data, it seems reasonable that we selected it as a representative result. But we presented the results of the subsets as well as that of the full dataset for all K's, allowing the reader to appreciate the subtle variation in outcomes at K's >10.

2.4. Additional notes on PCA results

Phylogenetic analyses at the individual level generally show tight clustering within populations, indicating that predefined population labels are usually informative about the genetic relationships among individuals at the level of geographical sampling that we have achieved (**Fig. S27**). This high degree of clustering is also apparent in individual level analyses of the first two principal components (PC) (**Fig. 2**). In each panel of Figure 2, population outliers have been identified, and then removed from the successive plot. In these plots of the first two PCs it is apparent that individuals from the same language family tend to cluster in close proximity to one another, and to their

geographic neighbors (with a few notable exceptions, which correspond very closely with the linguistic outliers identified in Figure 1). Notably, in **Fig. 2B**, the first PC generally orients individuals and populations according to their East-West coordinates within Eurasia, while the second PC corresponds, with very few exceptions, to a South to North axis. It is tempting to view the first PC, summarizing the greatest amount of variation, as reflecting the predominant and oldest cline of genetic variation established as modern humans first settled the Asian continent from Africa and the Middle East, and then (as reflected by the 2nd PC in **Fig. 2B**) gradually populated more northerly climes. However, it is likely that the detailed history of migrations is more complex, with various agricultural expansions (especially from North to South within Asia), and more recent movements in all directions affecting particularly the western periphery of Asia (*26*). Nevertheless, we see little evidence that these more recent events have greatly perturbed the geographic distribution of alleles that may have been established very early in the initial settlement of Asia. To some extent, this may be expected, since the demographic impact of each successive expansion would be blunted by admixture with existing human populations at their periphery.

Under the one-wave theory, one expects that the most geographically distant populations along the migration route will be the populations that are genetically most diverged from the CEU group. However, in the PCA plot, the northern populations who are most distant from Europe under a one-wave littoral theory (e.g. CHB, JPT) seem to be even closer to CEU than are the southern populations (**Fig. 2B**). This seems suggest that some degree of genetic contact with Europe and central or western Asia along a northern route is likely, contrary to the our claims about a single littoral route. However, we note that in the first PC, with or without the Yoruba, the CEU and the CHB/JPT are actually maximally distant. This is true also of the second PC with the Yoruba, but not when the Yoruba are removed. Given the intermediate position (both geographically and in the PC plots) of the Uyghur and Spiti (IN-TB), two populations with a known history of admixture among East Asian and Indo-European speaking populations, we suspect that any similarity along the second PC is due to this

historical gene flow – and not necessarily a deep ancestral connection. For example, the Uyghur (as also described in Li *et al.* 2008 Science 319:1100-1104) , like many Central Asian populations, have received recent gene flow both from populations tracing ancestry to East Asia but also to the Middle East/Europe. The position of the Uyghur does not support an ancient shared ancestry between European and (north) East Asian populations, as we observes previously (S*4, 48*). We also emphasize that the second and higher PC's explain very little of the total variance <= 1%, and that results can be very sensitive to the populations which are included in the analyses. For these reasons, we refrain from reaching strong conclusions on the basis of PC analysis alone.

2.5. Evaluation of the influence of ascertainment bias on inferences in this study

Ascertainment bias is likely to happen when SNPs are chosen from public database where the SNP discovery panels are often quite variable in size and composition; the bias could be further enlarged by choosing only SNPs that had been validated with high minor allele frequency (MAF) in population samples. In this section, we first evaluate the ascertainment bias in the Affymetrix 50k genotyping chip by comparing the observed allele frequency spectrum in 50k data and expected spectrum assuming a simple coalescent model in particular populations. We also compared the observed allele frequency spectrum of 50K SNP data with that of ENCODE region in particular populations. We further evaluate whether and how much the ascertainment bias affects the inferences in our study. The following analyses are all based on autosomal data. Previous work has shown that haplotype-based methods are less sensitive to the ascertainment protocols of individual SNPs (S*49*). We also found in our data that haplotype diversity is highest in Africans and decreases as the distance from Africa increases, which is consistent with a series of founder effects. In the evaluation of ascertainment bias, we focus on the individual SNPs but not haplotype.

2.5.1. Evaluation of the influence of ascertainment bias

Most analyses we carried out in this study, which are based primarily on tree-building algorithms rather than allele frequency distribution, thus in theory should not have been much affected by ascertainment bias. However, considering the fact that ascertainment bias exist in the data and its potential possibility of influence on history inferences, we analyzed the sub-datasets generated above by repeating the procedure that performed on original dataset. These analyses are to examine whether and how much ascertainment bias affects the inferences if a set of SNPs are chosen based on their frequencies in particular populations.

2.5.1.1. Evaluation of the influence on genetic distance estimation

We firstly investigated whether population genetic distances calculated from sub-datasets are significantly different with that calculated from the original dataset. F_{ST} matrix was estimated from 75 populations in subset1 data selected based on expected spectrum in YRI under coalescence model; **Figure S33** displayed a correlation relationship between F_{ST} matrices calculated from subset and full dataset. The overall correlation of F_{ST} between full dataset and sub-dataset is very high, indicated by high correlation coefficient ($r > 0.98$) and significant p-value ($p < 10^{-4}$), nonetheless, we do observe different F_{ST} distribution between full data and sub-datasets. For example, in sub-dataset of which SNPs were selected based on expected MAF spectrum in YRI under coalescent model (**Figure S33A**), all F_{ST} comparisons between African and nonAfrican deviate from the correlation line. F_{ST} values calculated from sub-dataset selected in YRI are generally higher than F_{ST} values calculated from full data for comparisons of YRI and non-African populations. This result indicated the genetic difference between YRI and non-African populations are larger. When SNPs were selected based on their MAF spectrum in CEU, the deviated F_{ST} comparisons are between CEU and the other populations (**Figure S33B**), with the genetic differences between CEU and Asian increased in sub-datasets. However, when SNPs were selected based on their MAF spectrum in CHB, there is

not obvious deviation (**Figure S33C**), but the overall F_{ST} values are larger in sub-dataset than that in full data. A similar pattern was observed in sub-datasets selected based on their MAF spectrum in ENCODE regions (**Figure S33E, F, G**), but the deviations are still stronger which, to a large extent, due to the MAF spectrum in ENCODE regions including much more low frequency SNPs compared with than in full Affymetrix 50K data.

2.5.1.2. Evaluation of the influence on tree topologies

The above analyses showed differences exist in distributions between full Affymetrix 50K data and sub-datasets with biased SNPs selected based on allele frequencies in single particular population, but it is not clear whether or how much the tree topologies are affected. We further analyzed 100 sub-datasets selected above based on expected spectrum in YRI under coalescence model and reconstructed a maximum likelihood tree (**Figure S34A**), maximum likelihood trees based on 100 sub-datasets selected in CEU (**Figure S34B**) and CHB (**Figure S34C**) were also reconstructed respectively. We also analyzed sub-datasets of which SNPs were selected in particular population based on their MAF spectrum in ENCODE regions, the maximum likelihood trees reconstructed from 100 sub-datasets selected in YRI, CEU and CHB were shown in **Figure S35A, B, C** respectively. Using the same procedure, maximum likelihood trees were also reconstructed from 100 sub-datasets selected based on expected allele frequency distribution in Malay Negritos and Philippine Negritos respectively, the results were shown in **Figure S36A, B**, respectively. In all cases, we do not see significant change of tree topologies and population grouping pattern compared with that reconstructed from the full dataset, and notably, the topologies and population grouping pattern of three maximum likelihood trees are also consistent. This result indicated that ascertainment bias does not invalidate the inferences based on tree topologies.

2.6. Additional notes on language replacement

Populations from the same linguistic group tend to cluster together, showing the expected correlation between genetic and linguistic distances, with the exception of eight populations with known or suspected histories of admixture or language replacement: the Uyghur (CN-UG), a Central Asian population in western China along the route of the ancient Silk Road connecting Europe to Asia; the Ladakhi (Spiti) (IN-TB), a Sino-Tibetan speaking population in India, south of the Himalayas; the Mon of Thailand (TH-MO); the Malaysian Negritos (MY-JH and MY-KS), with a likely history of language replacement that we discuss below; the Nasioi Melanesians (AX-ME), grouping with several eastern Indonesian populations known to have mixed with Papuan speaking populations to their east; and the Karen (TH-KA) and the Jinuo (CN-JN), both of which speak Sino-Tibetan languages but inhabit Southeast Asia and are surrounded primarily by the Austro-Asiatic, Tai-Kadai, and Hmong-Mien speaking populations among whom they cluster in the tree.

2.7. Additional notes on Taiwan Aborigines

A recent classification of Austronesian languages showing maximal diversity in the languages of Taiwan (*21*) has suggested this island as the ancestral “homeland” for Austronesian speaking populations throughout the Indo-Pacific. We sampled two populations (AX-AM/Ami and AX-AT/Atayal) representing two deeply differentiated Austronesian sub-families (Paiwanic and Atayalic) in Taiwan. STRUCTURE/*frappe* analysis (**Fig. S1-S26**) indicates that the two aboriginal populations of Taiwan share a common component with most other Austronesian speaking populations. In addition, the topology of the maximum-likelihood population tree (**Fig. 1**) seems to suggest that Taiwan aborigines may be derived from, rather than ancestral to other Austronesian populations, because they occupy central, rather than peripheral positions within the cluster of Austronesian speaking populations. This observation seems to contradict a

commonly cited Taiwan “homeland” hypothesis of Austronesian populations. Given a nearly total lack of prior autosomal data from Southeast Asian populations (*9, 10*), and conflicting evidence based on mtDNA analyses, some of which questions the Taiwan homeland story (*22, 23*), we believe our data should prompt a reexamination of hypotheses for the origins of the Austronesian languages and their speakers.

2.8. Additional notes on Indian populations

In all of our analyses, Indian populations showed considerable evidence of similarity to European populations (**Fig. 1, Fig. 2, S1~S26, S27, S28**), and in STRUCTURE/frappe results, Indian populations have a substantial contribution of 'European' ancestry (**Fig. S1~S26**). This is highly consistent with what we know about the introduction of Indo-European languages into both India and Europe. Our data therefore differ markedly from the results of Rosenberg et al. (S*50*), which posited India as a vast (yet entirely homogenous) reservoir of a unique component of human diversity found nowhere else on earth. The reasons for our differing results are not entirely obvious, but possibilities include: differing mutation rates or ascertainment biases in the SNP vs. microsatellite markers; differing population samples (theirs were from Indians resident in the U.S.A., ours were sampled in India); and our sample includes only one Dravidian speaking population, theirs includes 4 (although they also sample from 11 Indo-European speaking populations). Nearly all of our population samples were donated by members of high castes, and there is compelling historical and genetic data (Genome Res. **11**:994-1004) that the Indo-European migrants both established the caste system, and ensconced themselves in the highest castes. Finally, though we have no direct evidence for it, it is possible that the genotypes for the Indian samples in Rosenberg et al. (S*50*) were called differently than those of all the other populations, and this would certainly tend to group the Indians separately from all other populations. The Indian samples were genotyped as a group in 2004 (and possibly at another lab), while the other samples were genotyped in 2002. As Rosenberg et al. discuss (and made some statistical, but indirect and thus imperfect, efforts to correct), many changes in both the primer sequences and (crucially) fragment sizing software had changed between the two genotyping episodes, and

thus inconsistent allele-calling is a real possibility.

The relatively recent introduction to India of Indo-European languages and the genes of their speakers (which, as we now explicitly remark in the manuscript, is evident in our data) is unanimously accepted by nearly every student of Indian prehistory. Therefore, we discuss the pre-historical migration in Asia, we are not discussing the arrival of Indo-European speaking populations in India, Instead, we focus on the major entry to Southeast and East Asia. Our one- and two-wave models concern the settling of Southeast and Northeast Asia. The genetic proximity of Northeast Asian and European populations seen in earlier studies of classical markers has led to the idea of a second wave of migration predominantly to Northeast Asia – a wave that would also have contributed to or emanated from Europe. Our data do not show this relative similarity between Northeast Asian and European populations, leading us to question the evidence for a second major wave of migration into East Asia.

2.9. Addition notes on isolation by distance and pre-historical population divergence

2.9.1. Geographical distance versus genetic distance

Previous studies have hypothesized a serial founder effect originating in Africa by showing a relationship between genetic and geographic distances (*11, 24, 25*). We combined data for 19,934 common SNPs typed in 52 HGDP samples (*11*) and calculated F_{ST} (*26*) and great circle geographic distances from East Africa for the 126 populations. Our results confirmed previous observations of a linear increase in genetic distance with geographic distance. The PC analysis further emphasizes this geographic patterning of the populations (**Fig. 2**). Notably, in **Fig. 2B**, the first PC generally orients individuals and populations according to their East-West coordinates within Eurasia, while the second PC corresponds, with very few exceptions, to a South to North axis. This pattern is consistent with a serial founder effect during the initial peopling of Asia. The same pattern is echoed in the branching order of groups on the

population tree (**Fig. 1**), which shows a South-North pattern – from the Austronesian and Austro-Asiatic speaking populations in the extreme south, to the Tai-Kadai, Hmong-Mien, Sino-Tibetan, and, finally, the northernmost Altaic speaking populations.

2.9.2. IBD versus historical divergence

Although the branching pattern of population tree (**Fig. 1**, **Fig. S28**) showed a hierarchical splitting of ethnic or linguistic groups and indicated the possible pre-historical divergence with South-North migration of Asian populations, the alternative model of current divergence and equilibrium process such as isolation by distance (IBD) can also explain such a pattern. The expression “isolation by distance” was initially introduced by S. Wright (S*51, 52*), it indicates the tendency of populations to exchange genes with nearest neighbors, resulting in a greater genetic affinity between geographically closer groups and the likely occurrence of genetic differences between groups that are far apart because of genetic drift (S*53*). The models developed by Wright have been conceptually influential but have had little practical application. More popular have been the models of IBD developed by Malécot (S*54*) and by Kimura and Weiss (S*55*) in spaces of one or two dimensions, according to whether the migrating populations are supposed to live on a linear habitat (e.g., a group of islands placed along a line) or on a more common two-dimensional habitat. The approaches by Malécot and by Kimura and Weiss differ, but the qualitative predictions are alike. The one-dimensional models are consistent in showing an exponential decrease of the genetic similarity between two demes with their geographic distance (S*53*).

We used partial and multiple Mantel tests to simultaneously test pre-historical divergence effects and IBD effects. Partial Mantel regression was used to partition the effects of geographic structure and long-term divergence associated with possible pre-historical population splits. The general idea is that the IBD process occurs on a much smaller time-scale than long-term historical isolation or deep-time coalescence (S*23*).

The simple matrix correlation of genetic and geographic distance was 0.332 ($P < 0.0001$ with 10,000 permutations), consequently, about 11% of the variation in genetic distances can be attributed to geographic distances between pairs of populations; while correlation of genetic and clustering indicator matrix was 0.462 ($P < 0.0001$ with 10,000 permutations), thus about 21.3% of the variation in genetic distances can be attributed to pre-historical divergence of Asian populations. Partial correlation of genetic and geographic distance was 0.228 ($P < 0.0006$ with 10,000 permutations), after controlling for clustering indicator matrix; while partial correlation of genetic and clustering indicator matrix was 0.403 ($P < 0.0001$ with 10,000 permutations) after controlling for geography.

When the Mantel test was applied to the populations within each clade (cluster or group), the correlation between genetic and geographic distance generally decreased. For example, the correlation between genetic and geographic distance in Tai-Kadai group was 0.293 ($P = 0.208$ with 10,000 permutations); the correlation between genetic and geographic distance in Indian group was 0.135 ($P = 0.263$ with 10,000 permutations); in some groups, the correlation even reversed, for example, the correlation between genetic and geographic distance in Hmong-Mien group was -0.99 ($P = 0.168$ with 10,000 permutations), which was unexpected by IBD model. Therefore, the relationship between these populations and those on the other groups is not fully additive and these groups are probably subject to different evolutionary processes (S*23*).

Overall about 16.2% of the variation in the genetic distances (F_{ST}) could be attributed to pre-historical divergence alone, whereas only 5.2% of the variation in genetic distances could be attributed to IBD. In other words, spatial patterns in genetic distances are much better explained by differences between groups of populations than by similarity among adjacent local populations within these groups. However, as expected, there is a large overlap between the two processes, the long-term divergence binary matrix is also structured in geographic space ($r = 0.301$; $P < 0.0001$ with 10,000 permutations), in such a way that it is not possible to entirely partition population divergence between historical and contemporary processes such as IBD (S*23*).

We further carried out a simulation study under isolation by distance (IBD) to explore whether IBD could alone generate the patterns that were observed. Our simulation results showed two-dimensional model of IBD could not generate the branching patterns of population trees observed in this study; one-dimensional model (gene flow along south-north way) of IBD could generate similar tree branching patterns observed in East Asian populations with a few exceptions, but was not compatible with the distribution of herterozygosity pattern observed in East Asian populations, i.e. herterozygosity decreasing from south to north. When admixture of West Eurasian ancestry in Southeast Asia was simulated in one-dimensional IBD, the observed diversity pattern could to some degree be mimicked, however, the phylogeny of group private haplotypes could not be recovered, i.e. the East Asian private haplotypes and West Eurasian private haplotypes cluster together firstly since East Asian private haplotypes initially derived from West Euroasian in simulation under “pincer model” (S*56*); while in real data East Asian private haplotypes and Southeast Asian private haplotypes cluster firstly. Therefore, both two-dimensional and one-dimensional IBD effects could not totally explain the observed pattern in current data.

On balance, although we could not totally ignore the contribution of IBD, our data show strong signal of the effect due to pre-historical population divergence.

2.10. Evidence of southern origins of East Asian populations and South-to-North migration

Origin of East Asian populations has been debatable in human evolutionary studies, here, after analyzing genome-wide data in adequate Asian samples, we provide evidence that supports the south origin of East Asian and South-to-North migration, i.e. East Asian initially most likely derived from Southeast Asian populations, with contribution from north in later time.

2.10.1. Topology of maximum likelihood tree of populations

Using 42,793 SNPs whose ancestral allele states are known, we reconstructed a maximum likelihood tree of 75 human populations with most recent common ancestor of humans as an out group (**Fig. 1**). East Asian populations cluster together with Southeast Asian populations and are the last split of branches, the topology and branching pattern of the tree support the south origin of East Asian populations. A maximum likelihood tree of 126 world-wide populations with CEPH-HGDP samples included (**Fig. S28**) also supports this idea.

2.10.2. Distance of STRUCTURE/*frappe* components

At *K*=2 (**Fig. S1**, **Fig. S14**) and *K*=3 (**Fig. S2**, **Fig. S15**), all Southeast (SE) and East Asian (EA) samples are united by predominant membership in a common cluster, with the other cluster(s) corresponding largely to Indo-European (IE) and African (AF) ancestries. At *K* = 4 (**Fig. S3**, **Fig. S16**), the new component accounts for shared ancestry of all SE samples and dominated in both Negrito and Papuan samples, the net nucleotide distance (S*33, 34*) between SE and EA (0.020) inferred from STRCTURE components are much less than any other pair comparisons (0.062 for SE-AF, 0.065 for EA-AF, 0.049 for IE-AF, and 0.032 for both SE-IE and EA-IE), which suggest SE and EA shared the most recent common ancestral origins.

2.10.3. Topology of STRUCTURE/*frappe* component tree

We reconstructed a phylogenetic tree relating the clusters based on allele frequencies in each cluster inferred from the STRUCTURE/*frappe* analysis. Phylogenetic relationships of these clusters (referred to as the “component tree”), given their statistical independence, should reveal an evolutionary history that is less perturbed by recent gene flow and admixture than is a population phylogeny. With African component as out group, the split of East Asian and Southeast Asian components is the latest one, thus supports the idea of East Asian populations derived

from Southeast Asian populations, and again, the tree topology and branching pattern support South-to-North migration history.

2.10.4. Distribution of samples in PCA plots

Distribution of Asian samples in PCA plot (**Fig. 2D**) consists the South-North spatial pattern, strong correlation of PC1 and latitudes supports the South-North migration.

2.10.5. Geographical distribution of genetic diversities

Generally speaking, later derived populations have less genetic diversity; the decreasing trend of geographical distribution of genetic diversity indicates the migration directions. Distribution of haplotype diversities of Southeast and East Asian populations showed a South-to-North decreasing trend with strong correlation between diversities and latitudes (**Fig. 3A, Fig. S37**), strongly suggesting the South-to-North migration.

2.10.6. Haplotype sharing proportions

We conducted haplotype-based analysis to examine the contribution of other source of haplotypes to East Asian (EA) gene pool. Due to the different marker densities and population samples in PanAsia data and combined data (see Methods), we considered the two data sets separately. Population/group private haplotypes were identified using methods describes above.

For PanAsia data, we examined the contribution Southeast Asian (SE) and Indians (IN) to East Asian (EA) gene pool. EA populations were grouped as Japanese (**JP**, including JP-RK, JPT and JP-ML), Korean (**KR**, including KR-KR), Han Chinese (**HAN**, including CHB, CN-SH, CN-GA, TW-HA, TW-HB and SG-CH), and Southern Chinese minorities (**S-CM**, including CN-HM, CN-CC, CN-JI, CN-WA and CN-JN). Haplotypes of each group were compared with that of SE and IN, and were classified

as HSa (IN private), HSb (EA private), HSc (sharing by all groups), HSd (SE private). The distribution of proportions of each haplotype class in each group, when frequency was not considered (type only) is shown in **Figure S38**. More than 90% of East Asian haplotypes could be found in Southeast Asian populations and East Asian gene pool is constituted of about 65% of SE private haplotypes and less than 2.5% of IN private haplotypes.

For combined data set, we examined the contribution of Southeast Asian (SE) and Central-South Asian (CSA) to East Asian (EA) gene pool. EA populations were grouped as Yakut (**YKT**, including Yakut), Northern Chinese minorities (**N-CM**, including Xibo, Mongola, Oroqen, Daur, Hezhen and Tu; the two Uyghur populations were not included), Northern Han Chinese (**N-HAN**, including CHB and Han-NChina), Japanese and Korean (**JP-KR**, including Japanese, KR-KR, JP-ML, JPT and JP-RK), Southern Han Chinese (**S-HAN**, including Han, CN-SH, TW-HA, TW-HB, CN-GA and SG-CH), and Southern Chinese minorities (**S-CM**, including Tujia, Yi, Miao, She, CN-HM, Naxi, AX-AT, CN-CC, AX-AM, CN-WA, Lahu, CN-JN, Dai and CN-JI). Haplotypes of each group were compared with that of CSA and SE, and were classified as HSa (CSA private), HSb (EA private), HSc (sharing by all groups), HSd (SE private). The distribution of proportions of each haplotype class in each group, when frequency was not considered (type only) is shown in **Figure 3B**. More than 90% of East Asian haplotypes could be found in Southeast Asian populations and East Asian gene pool is constituted of about 50% of Southeast Asian private haplotypes and 5% of Central-South Asian private haplotypes.

The above results indicate the contribution of SE to EA modern gene pool is major, while the contribution of CSA is minor, except in some of populations such as Uyghur populations reside in Northwest of China where we observed recent significant gene flow from Central Asia or Europe (S*4, 48*), this is also the reason we did not include the two Uyghur populations in the above analyses.

2.10.7. Phylogeny of group private haplotypes

We further reconstructed phylogenetic relationship of group private haplotypes (see Methods). Phylogeny of group private haplotypes showed EA has a closest relationship with SE, thus supports the idea EA derived directly from SE, the contribution from other sources (e.g. CSA) was minor and could have occurred in later time.

2.11. Peopling of Asia: one-wave versus two-wave hypothesis

According to Cavalli-Sforza *et al*. (S*57*), anatomically modern humans (also called *Homo sapiens sapiens*) spread into Asia through two routes. "The first was a southern route, perhaps along the coast to south and Southeast Asia, from where it bifurcated north and south. In the south, these modern humans reached Oceania between 60 and 40 kya, whereas the northern expansion later reached China, Japan and eventually America (this might represent the second migration to America, associated with the NaDene languages, postulated by Greenberg). The second was a central route through the Middle East, Arabia or Persia to central Asia, from where migration occurred in all directions reaching Europe, east and northeast Asia about 40 kya, after which the first and principal migration to America suggested by Greenberg occurred not later than 15 kya." This hypothesis was based almost entirely on classical protein and blood group data from a handful of markers which resulted in phylogentic tree topologies appearing to show that populations in Northeast Asia are more similar to European populations than they are to populations living in Southeast Asia.

Based on hypothesis of Cavalli-Sforza *et al.* and our observations on Asian Negritos, we constructed three models which are testable, as illustrated in **Figure S29** and described in Methods. Models 1 and Model 2 are both consistent with the scenarios hypothesized by Cavalli-Sforza *et al*, which we call "two-wave" hypothesis, while Model 3 suggests a "one-wave" hypothesis, i.e. the majority of the gene pool in Asia (the part that gave rise to all modern East Asian and Southeast Asian populations)

was derived from a single initial entry of modern humans into the subcontinent.

In the following sub-sections, in addition to a phylogenetic tree topology which contrasts sharply with Cavalli-Sforza's older trees based on much less data, we list some additional evidence in support of the one-wave hypothesis; or more precisely, the idea that the majority of the gene pool in Asia (the part that gave rise to East Asian and Southeast Asian populations) was derived from a single initial entry of modern humans into the subcontinent.

2.11.1. Topology of population trees

As the topology of a maximum likelihood tree of 75 populations (**Fig. 1**) showed, all Negrito populations cluster together with Southeast Asian populations and are the last split of branches, the topology and branching pattern of the tree support the south origin of East Asian populations. A maximum likelihood tree of 126 world-wide populations with CEPH-HGDP samples included (**Fig. S28**) also supports this idea.

2.11.2. Topology of STRUCTURE/*frappe* component tree

We reconstructed a phylogenetic tree relating the clusters based on allele frequencies in each cluster inferred from the STRUCTURE/*frappe* analysis. Phylogenetic relationships of these clusters (referred to as the "component tree"), given their statistical independence, should reveal an evolutionary history that is less perturbed by recent gene flow and admixture than is a population phylogeny. With African component as out group, the split of East Asian and Southeast Asian components is the latest one, thus supports the idea of East Asian populations derived from Southeast Asian populations.

The overall pattern of this component tree is similar to that of the population tree (**Fig. 1**) with a few revealing exceptions. The component we associate with Austronesian speakers now groups with the mainland East Asian components, consistent with the idea that this language family expanded from mainland East Asia –

possibly following the development of rice agriculture, as has been previously hypothesized on archeological and linguistic grounds (S*42*). The Negrito and Papuan groups are now closer to the root of the East Asian and Southeast Asian clades, with the European and Indian groups positioned outside the clade. This suggests that the divergence of the Negrito groups and the other Asian populations occurred after the divergence of Asian and European populations.

2.11.3. Phylogeny of group private haplotypes

Private haplotypes of Negrito (NG), Asian (AS) and European (EUR) were identified and phylogenetic tree of group private haplotypes was reconstructed with same method described in **2.11.6**. Phylogeny of group private haplotypes indicated NG and AS has the closest relationship, thus suggesting divergence of non-Pygmy-Asian/Asian Pygmies was not earlier than that of Asian/European, this result further implying the majority of the gene pool in Asia (the part that gave rise to East Asian and Southeast Asian populations) was derived from a single initial entry of modern humans into the subcontinent.

2.11.4. Simulation results

The topology of our population trees, both with or without the data from additional European and Asian populations in (S*3*) provide little support for the two-wave model, and appear more consistent with a single major peopling of Asia (**Fig. 1, S28**) – nor does the population tree of ref (S*3*) based on all 642,690 SNPs. The rather surprising tree topology that first led to the suggestion of a two-wave model, in which populations in Northeast Asia were more similar to populations inhabiting Europe than to populations in Southeast Asia is not seen with the much larger number of DNA variants analyzed in recent studies. However, there is still a formal possibility that high levels of gene flow from neighboring populations into the Negritos could have contributed to the observed tree topology, which places the Negritos within the monophyletic grouping of all other Asian populations within our sample. We therefore

performed simulations to estimate the level of gene flow from neighboring populations that would have been required to change the tree topology. We examined three relevant models (**Fig. S29**) based on the two-wave and one-wave hypotheses and applied forward time simulations (see above descriptions). Results of the forward time simulations (**Fig. S30**) indicate that the two-wave model is only compatible with the empirical data if gene flow to Negrito populations has been extensive, i.e., if more than half of the chromosomes in the Negrito populations resulted from recent admixture with neighboring populations. Although such a high degree of gene flow (> 50%) seems unlikely particularly in light of the phenotypic differences between Negritos and other populations, we did observe such high degree of general Asian gene contribution in some of Philippine Negrito populations, for example, and general Asian components are summed together 61.0% for PI-AG and 58.7% for PI-IR. The average proportion of general Asian components is 44.4% in Philippine Negritos, and 10.6% in Malaysia Negritos. There could be some mechanism of natural or sexual selection acting to preserve this phenotype in the presence of considerable admixture from later migrants.

In addition, at K=2 in STRUCTURE/*frappe* results (**Fig. S1, S14**), East Indonesian and Negrito populations show similarity to the YRI. This result seems potentially suggests a second early migration, ancestral to Negritos and some Austronesians, that has left detectable similarity to Africans despite admixture with descendants of subsequent migrations. However, there is very little evidence that any non-African populations (including SE Asian Negritos, termed “Orang Asli” in the paper of Macaulay et al. Science (2005) **308**:1034 – 1036) derive from other than a small number of initial out-of-Africa events some 50,000 to 150,000 years ago. We would speculate that this very tentative connection among Negrito and African populations could be explained if the Negrito populations required fewer adaptive changes to life in tropical latitudes similar to the ones their ancestors had inhabited in Africa. East Asian populations inhabiting more northern climates, by contrast, are likely to have experienced novel selection pressures as they moved into new latitudes and

environments. It would not be surprising if such adaptations significantly altered allele frequencies throughout much of the genome, via linkage disequilibrium with selected variants.

Furthermore, the placement of the AX-ME near the MY-JH and MY-KS in the PCA plot (**Fig. 2B**) provides a similar result to the STRUCTURE analysis. We believe this similarity of the AX-ME and the Malaysian Negritos (who also share some phenotypic similarity) is consistent with, and in fact bolsters the one-wave hypothesis, in which modern humans are thought to have first entered Southeast Asia along a mostly coastal route and continued rapidly to modern day Australia, Papua, and neighboring Melanesian Islands. These populations would be the most direct descendants of the initial modern humans, with less need to adapt to changing climate and a non-tropical environment. Descendants of these initial Southeast Asian populations appear then to have moved, perhaps more gradually, to the north of the continent, with significant adaptations occurring to the local climate and environment, which changes more sharply with latitude than longitude.

2.11.5. Final comments

When the genetic data in this study are considered together with the geographical distribution of the clusters and archeological and linguistic information, we propose the following model of human migrations in Asia. The initial entry is likely to have followed a southern route to Southeast Asia (S*58*). From there, populations gradually moved north, adapting to climatic and local selective pressures. Subsequently, and particularly with the development of agriculture as a stimulus, populations in northern and central East Asia may have expanded southwards, altering the physical characteristics of the original inhabitants.

3. References

S1. *Nature* **426**, 789 (Dec 18, 2003).

S2. K. A. Frazer *et al.*, *Nature* **449**, 851 (Oct 18, 2007).

S3. J. Z. Li *et al.*, *Science* **319**, 1100 (Feb 22, 2008).

S4. S. Xu, L. Jin, *Am J Hum Genet* **83**, 322 (Sep 12, 2008).

S5. G. C. Kennedy *et al.*, *Nat Biotechnol* **21**, 1233 (Oct, 2003).

S6. C. Zhang *et al.*, *Bioinformatics* **22**, 2122 (Sep 1, 2006).

S7. S. Schneider, D. Roessli, L. Excoffier, *Genetics and Biometry Lab, Dept. of Anthropology, University of Geneva.*, (2000).

S8. S. Wright, *Nature* **166**, 247 (Aug 12, 1950).

S9. M. Slatkin, *Genet Res* **58**, 167 (Oct, 1991).

S10. B. Su *et al.*, *Am J Hum Genet* **65**, 1718 (Dec, 1999).

S11. J. L. Mountain, L. L. Cavalli-Sforza, *Am J Hum Genet* **61**, 705 (Sep, 1997).

S12. A. L. Price *et al.*, *Nat Genet* **38**, 904 (Aug, 2006).

S13. B. S. Weir, W. G. Hill, *Annu Rev Genet* **36**, 721 (2002).

S14. M. Nei, *Am. Nat.* **106**, 283 (1972).

S15. M. Nei, F. Tajima, Y. Tateno, *J Mol Evol* **19**, 153 (1983).

S16. N. Saitou, M. Nei, *Mol Biol Evol* **4**, 406 (Jul, 1987).

S17. S. Kumar, K. Tamura, M. Nei, *Brief Bioinform* **5**, 150 (Jun, 2004).

S18. J. Felsenstein, *Am J Hum Genet* **25**, 471 (Sep, 1973).

S19. J. Felsenstein, *Cladistics* **5**, 164 (1989).

S20. S. Ramachandran *et al.*, *Proc Natl Acad Sci U S A* **102**, 15942 (Nov 1, 2005).

S21. N. A. Rosenberg *et al.*, *PLoS Genet* **1**, e70 (Dec, 2005).

S22. M. Jakobsson *et al.*, *Nature* **451**, 998 (Feb 21, 2008).

S23. M. P. Telles, J. A. Diniz-Filho, *Genet Mol Res* **4**, 742 (2005).

S24. S. Santos, H. Schneider, I. Sampaio, *Genet. Mol. Biol.* **26**, 151 (2003).

S25. B. F. J. Manly, *The statistics of natural selection*. (Chapman & Hall, London, UK., 1985).

S26. B. F. J. Manly, *Randomization, bootstrp and Monte Carlo methods in biology*. (Chapman & Hall, London, UK., 1997).

S27. R. R. Sokal, N. L. Oden, J. Walker, D. M. Waddell, *J. Hum. Evol.* **32**, 501 (1997).

S28. F. M. Rodrigues, J. A. Diniz-Filho, L. A. M. Bataus, R. P. Bastos, *Genet. Mol. Biol.* **25**, 435 (2002).

S29. B. F. J. Manly, *Res. Popul. Ecol.* **28**, 201 (1986).

S30. B. A. Hawkins, E. E. Porter, J. A. F. Diniz-Filho, *Ecology* **84**, 1608 (2003).

S31. P. Legendre, L. Legendre, *Numerical ecology.*, (Elsevier, Amsterdam, Holland, 1998).

S32. R. Leblois, A. Estoup, F. Rousset, *Mol Ecol Res*, doi:10.1111/j.1755 (2008).

S33. J. K. Pritchard, M. Stephens, P. Donnelly, *Genetics* **155**, 945 (Jun, 2000).

S34. D. Falush, M. Stephens, J. K. Pritchard, *Genetics* **164**, 1567 (Aug, 2003).

S35. H. M. Cann *et al.*, *Science* **296**, 261 (Apr 12, 2002).

S36. G. A. Huttley, M. W. Smith, M. Carrington, S. J. O'Brien, *Genetics* **152**, 1711 (Aug, 1999).

S37. D. E. Reich *et al.*, *Nature* **411**, 199 (May 10, 2001).

S38. M. Laan, S. Paabo, *Nat Genet* **17**, 435 (Dec, 1997).

S39. M. Jakobsson, N. A. Rosenberg, *Bioinformatics* **23**, 1801 (Jul 15, 2007).
S40. N. A. Rosenberg *et al.*, *Science* **298**, 2381 (Dec 20, 2002).
S41. N. A. Rosenberg *et al.*, *Genetics* **159**, 699 (Oct, 2001).
S42. J. Diamond, P. Bellwood, *Science* **300**, 597 (Apr 25, 2003).
S43. H. Tang, J. Peng, P. Wang, N. J. Risch, *Genet Epidemiol* **28**, 289 (May, 2005).
S44. P. Scheet, M. Stephens, *Am J Hum Genet* **78**, 629 (Apr, 2006).
S45. S. Myers, L. Bottolo, C. Freeman, G. McVean, P. Donnelly, *Science* **310**, 321 (Oct 14, 2005).
S46. S. Xu, W. Jin, L. Jin, *Mol Biol Evol (doi:10.1093/molbev/msp130)*, (Jun 29, 2009).
S47. M. F. Hammer *et al.*, *J Hum Genet* **51**, 47 (2006).
S48. S. Xu, W. Huang, J. Qian, L. Jin, *Am J Hum Genet* **82**, 883 (Apr, 2008).
S49. G. Hellenthal, A. Auton, D. Falush, *PLoS Genet* **4**, e1000078 (May, 2008).
S50. N. A. Rosenberg *et al.*, *PLoS Genet* **2**, e215 (Dec, 2006).
S51. S. Wright, *Genetics* **28**, 114 (Mar, 1943).
S52. S. Wright, *Genetics* **31**, 39 (Jan, 1946).
S53. L. L. Cavalli Sforza, P. Menozzi, A. Piazza, *The history and geography of human genes*. (Princeton University Press, Princeton, New Jersey, 1993), pp. 52.
S54. G. Malécot, *Les Mathematiques de L'Hérédité*. (Masson, Paris, 1948).
S55. M. Kimura, G. H. Weiss, *Genetics* **49**, 561 (Apr, 1964).
S56. Y. C. Ding *et al.*, *Proc Natl Acad Sci U S A* **97**, 14003 (Dec 5, 2000).
S57. L. L. Cavalli-Sforza, M. W. Feldman, *Nat Genet* **33 Suppl**, 266 (Mar, 2003).
S58. P. Mellars, *Science* **313**, 796 (Aug 11, 2006).

4. Supplementary Tables

Table S1. Analysis of molecular variance (AMOVA).

Table S2. Institutions that performed the genotyping.

Table S3. Data quality control for samples.

Table S4. Details of SNP filtering.

Table S1. Analysis of molecular variance (AMOVA).

Sample	Number of groups	Number of populations	Variance components and 95% confidence intervals (%)		
			Within populations	Among populations within groups	Among groups
World		75	94.1 (94.0, 94.2)	5.9 (5.8, 6.0)	
Geographical region[a]	5	75	92.7 (92.6, 92.8)	3.3 (3.1, 3.5)	4.0 (3.9, 4.1)
Asia		72	95.6 (95.5, 95.6)	4.4 (4.4, 4.5)	
Asia	3	72	94.8 (94.8, 94.9)	3.3 (3.2, 3.5)	1.8 (1.8, 1.9)
East Asia		17	98.1 (98.1, 98.2)	1.9 (1.8, 1.9)	
SE Asia		46	95.4 (95.4, 95.5)	4.6 (4.5, 4.6)	
South Asia		9	97.8 (97.7, 97.9)	2.2 (2.1, 2.3)	
Language Family	10	75	93.6 (93.5, 93.7)	2.9 (2.7, 3.1)	3.5 (3.4, 3.6)
Altaic		5	98.6 (98.5, 98.7)	1.4 (1.3, 1.5)	
Sino-Tibetan		9	98.8 (98.7, 98.8)	1.2 (1.2, 1.3)	
Hmong-Mien		3	98.4 (98.3, 98.6)	1.6 (1.4, 1.7)	
Tai-Kadai		6	99.3 (99.2, 99.3)	0.7 (0.7, 0.8)	
Austro-Asiatic		9	93.5 (93.3, 93.7)	6.5 (6.3, 6.7)	
Austro-Asiatic[b]		7	94.6 (94.5, 94.6)	5.5 (5.4, 5.5)	
Austronesian		31	96.4 (96.3, 96.4)	3.6 (3.6, 3.7)	
Austronesian[c]		26	97.4 (97.3, 97.4)	2.6 (2.6, 2.7)	
Indo-European		8	96.5 (96.4, 96.6)	3.5 (3.4, 3.6)	
Dravidian		2	99.8 (99.7, 99.9)	0.2 (0.1, 0.3)	
Negritos	2	7	89.2 (89.1, 89.3)	6.9 (6.7, 7.1)	3.9 (3.8, 4.0)
Philippine Negrito[d]		5	89.8 (89.8, 89.9)	10.2 (10.1, 10.3)	
Malaysian Negrito[e]		2	96.8 (96.8, 96.9)	3.2 (3.1, 3.3)	

a: 75 populations were divided into 5 groups according to their geographical locations, i.e. East Asia, Southeast Asia (SE Asia), South Asia (India), Europe and Africa;

b: Austro-Asiatic group with 2 Negrito populations (Malaysian Negritos, see e) removed;

c: Austronesian group with 5 Negrito populations (Philippine Negritos, see d) removed;

d: Philippine Negrito group consists of 5 Philippine Negrito populations, PI-AE, PI-AG, PI-AT, PI-MW, PI-IR.

e: Malaysian Negrito group consists of 2 Malaysian Negrito populations, MY-JH and MY-KS;

Table S2. Institutions that performed the genotyping.

Country	Institution that performed genotyping	abbreviation
China	Chinese National Human Genome Center, Shanghai	CHGS
India	Institute of Genomics and Integrative Biology, New Delhi	IGIB
Japan	University of Tokyo	UT
Korea	Center for Genome Science, Korea National Institute of Health, Seoul	KNIH
Malaysia	Universiti Sains Malaysia, Kubang Kerian	USM
Singapore	Genome Institute of Singapore	GIS
Taiwan	Institute of Biomedical Sciences, Academia Sinica, Taipei	AST
USA	Affymetrix, Inc.	AFFX

Table S3. Data quality control for samples.

ID	Ethnicity	Genotyping Ctr.	WGA	# attempted	duplicates	DM < 90%	BRLMM < 90%	N
AX-AM	Ami	AFFX	No	10	0	0	0	10
AX-AT	Atayal	AFFX	No	10	0	0	0	10
AX-ME	Melanesian	AFFX	No	5	0	0	0	5
CN-CC	Zhuang	CHGS	No	26	0	0	0	26
CN-GA	Han	GIS	No	30	0	0	0	30
CN-HM	Hmong	CHGS	No	26	0	0	0	26
CN-JI	Jiamao	GIS	No	31	0	0	0	31
CN-JN	Jinuo	UT	No	43	14	0	0	29
CN-SH	Han	CHGS	No	26	0	5	0	21
CN-UG	Uyghur	CHGS	No	26	0	0	0	26
CN-WA	Wa	CHGS	No	56	0	0	0	56
ID-AL	Alorese	GIS	No	19	0	0	0	19
ID-DY	Dayak	GIS	No	18	0	5	1	12
ID-JA	Javanese	GIS	No	34	0	0	0	34
ID-JV	Javanese	GIS	No	19	0	0	0	19
ID-KR	Batak Karo	GIS	No	18	0	1	0	17
ID-LA	Lamaholot	GIS	No	20	0	0	0	20
ID-LE	Lembata	GIS	No	19	0	0	0	19
ID-ML	Malay	GIS	No	16	0	3	1	12
ID-MT	Mentawai	GIS	No	16	0	1	0	15
ID-RA	Manggarai	GIS	No	18	0	1	0	17
ID-SB	Kambera	GIS	No	20	0	0	0	20
ID-SO	Manggarai	GIS	No	19	0	0	0	19
ID-SU	Sundanese	GIS	No	25	0	0	0	25
ID-TB	Batak	GIS	No	20	0	0	0	20
ID-TR	Toraja	GIS	No	20	0	0	0	20
IN-DR	Upper caste (Brahmin)	IGIB	No	25	0	1	0	24
IN-EL	Upper Caste (Kayastha)	IGIB	No	21	0	5	0	16
IN-IL	Upper caste (Vashiya)	IGIB	No	23	0	8	0	15
IN-NI	Tharu (Himalyan Tribe)	IGIB	No	24	0	4	0	20
IN-NL	Upper caste (Brahmin)	IGIB	No	24	0	9	0	15
IN-SP	Upper caste (Vashiya)	IGIB	No	25	1	1	0	23
IN-TB	Ladakhi Buddhist	IGIB	No	25	0	2	0	23
IN-WI	Bhil (Northwest Tribe)	IGIB	No	25	0	0	0	25
IN-WL	Upper caste (Brahmin)	IGIB	No	19	0	5	0	14
JP-ML	Japanese	UT	No	72	0	1	0	71
JP-RK	Ryukyuan	UT	No	58	0	9	0	49
KR-KR	Korean	KNIH	No	97	7	0	0	90
MY-BD	Bidayuh	GIS	No	50	0	0	0	50
MY-JH	Negrito	GIS	No	50	0	0	0	50
MY-KN	Malay	USM	No	19	0	1	0	18
MY-KS	Negrito	GIS	No	30	0	0	0	30
MY-MN	Malay	USM	No	20	0	0	0	20
MY-TM	Proto-Malay	GIS	No	50	0	1	0	49
PI-AE	Agta	GIS	Yes	27	0	15	4	8
PI-AG	Aeta	GIS	Yes	28	0	16	4	8
PI-AT	Ati	GIS	Yes	33	0	9	1	23
PI-IR	Iraya	GIS	Yes	22	0	11	2	9
PI-MA	Manobo	GIS	Yes	29	0	9	2	18
PI-MW	Mamanwa	GIS	Yes	32	0	8	5	19
PI-UB	Urban	GIS	No	20	0	0	0	20
PI-UI	Urban	GIS	No	20	0	0	0	20
PI-UN	Urban	GIS	No	20	0	1	0	19
SG-CH	Chinese	GIS	No	30	0	0	0	30
SG-ID	Southern India origin	GIS	No	30	0	0	0	30
SG-MY	Malay	GIS	No	30	0	0	0	30
TH-HM	Hmong	GIS	No	20	0	0	0	20
TH-KA	Karen	GIS	No	20	0	0	0	20
TH-LW	Lawa	GIS	No	19	0	0	0	19
TH-MA	Mlabri	GIS	No	19	0	1	0	18
TH-MO	Mon	GIS	No	19	0	0	0	19
TH-PL	Palong	GIS	No	20	0	2	0	18
TH-PP	Plang	GIS	No	20	0	2	0	18
TH-TK	Tai Kern	GIS	No	20	0	2	0	18
TH-TL	Tai Lue	GIS	No	21	0	1	0	20
TH-TN	H'Tin	GIS	No	18	0	0	0	18
TH-TU	Tai Yuan	GIS	No	20	0	0	0	20
TH-TY	Tai Yong	GIS	No	20	0	2	0	18
TH-YA	Yao	GIS	No	19	0	0	0	19
TW-HA	Han	AST	No	48	0	0	0	48
TW-HB	Han	AST	No	32	0	0	0	32
			TOTALS	**1903**	**22**	**142**	**20**	**1719**

Table S3 Note:

QC data is shown for each population. The genotyping center at which the typing was done is shown, as well as whether the template DNA had undergone whole-genome amplification (WGA). The number of samples attempted is shown, together with the number of samples that were removed because they were duplicated, or because either their DM or BRLMM call-rates were below 90%. The final sample size after all exclusions (N) is also shown.

Table S4. Details of SNP filtering.

SNPs removed	Filter Description	SNPs remaining
0	SNPs genotyped on the Affymetrix 50k Xba	58960
389	SNP call rate < 90%	58571
2546	Intersection of PASNP SNP set with downloaded Hapmap genotypes	56025
1189	Chromosome X SNPs	54836
42	Unmapped in Affymetrix annotation file(Mapping50K_Xba240.na21.annot)	54794

5. Supplementary Figures

Figure S1 Estimated population structure from the full data set (Full) and 10 subsets of the data (S1-S10) (K=2).

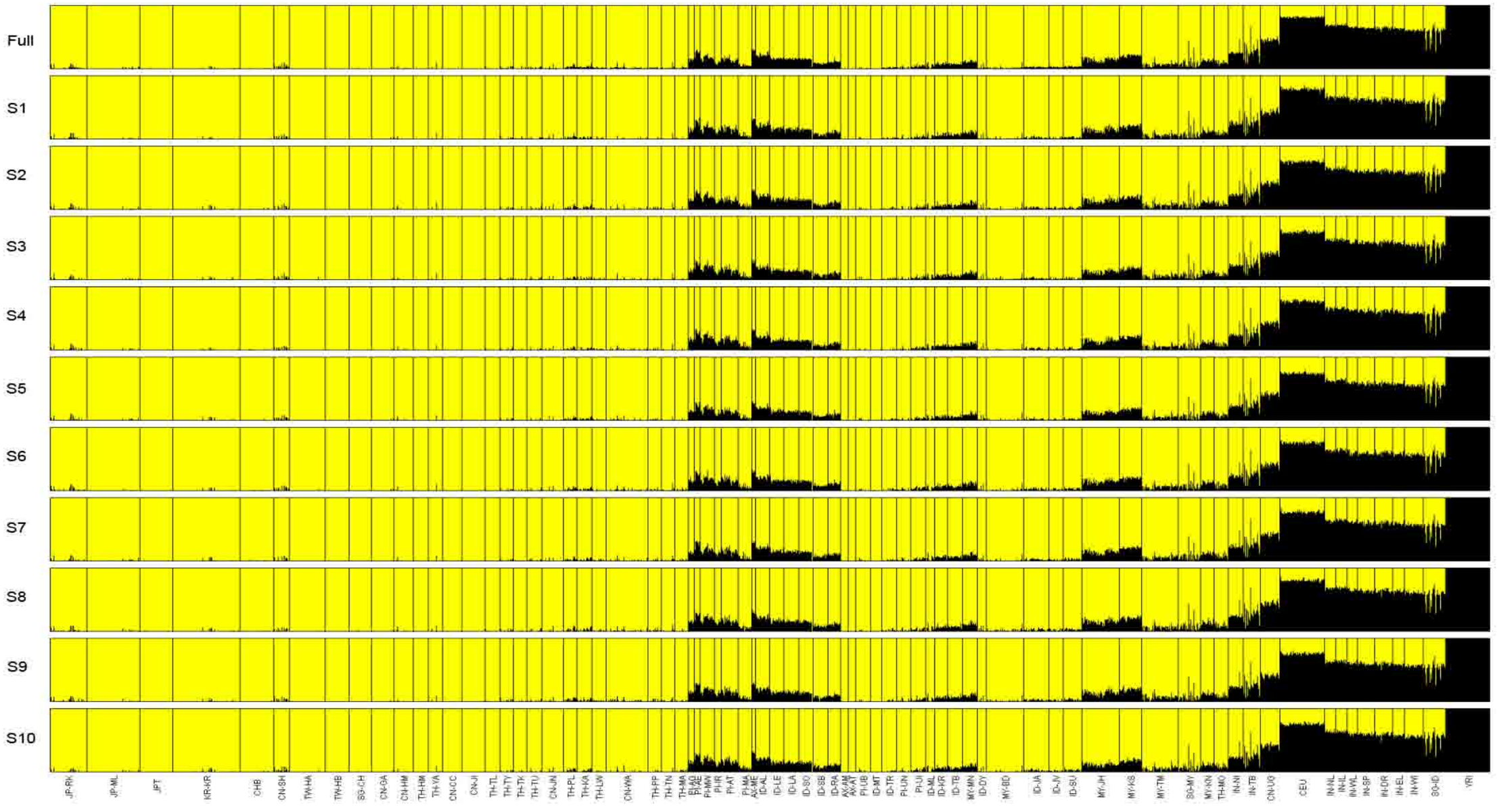

Figure S2 Estimated population structure from the full data set (Full) and 10 subsets of the data (S1-S10) (K=3).

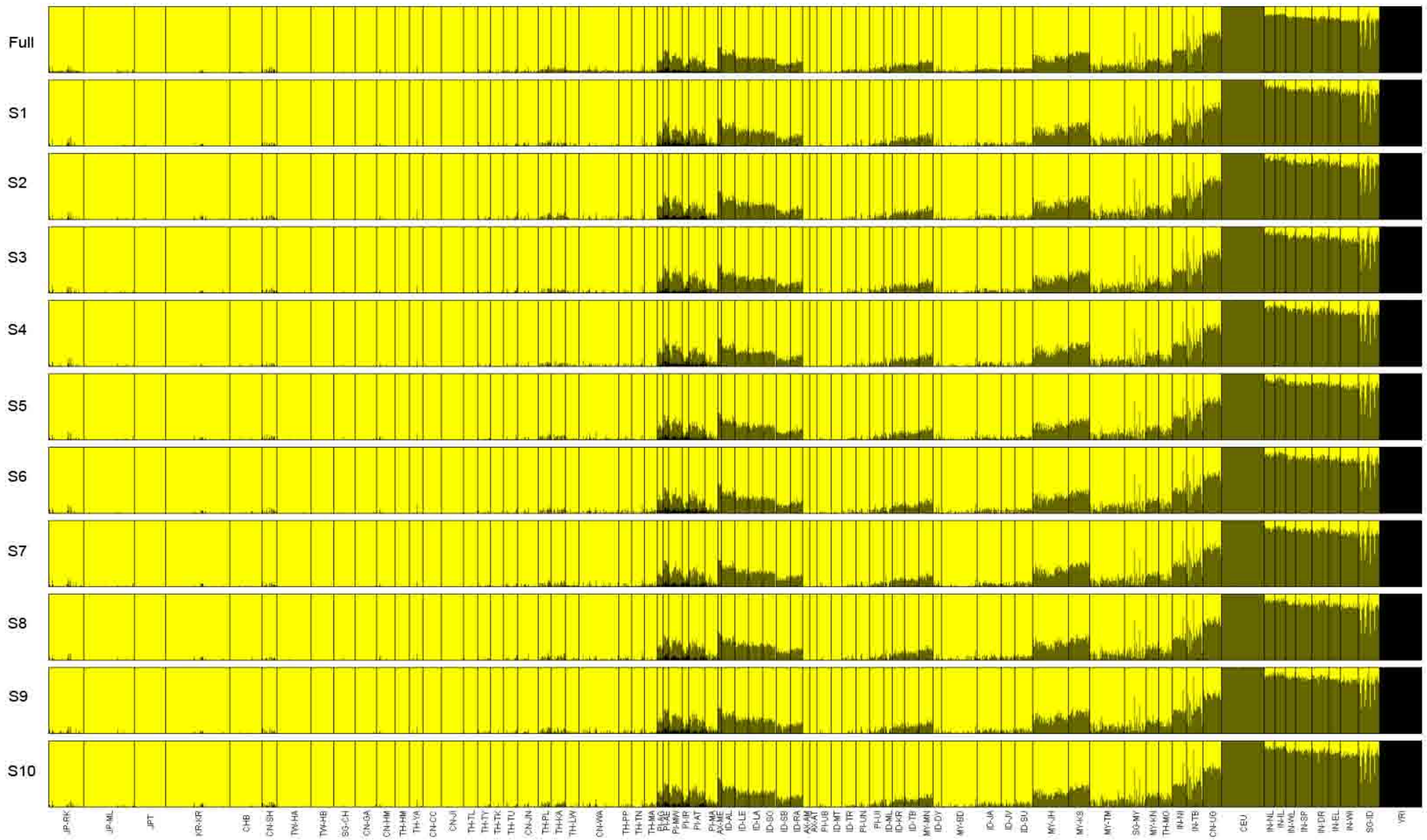

Figure S3 Estimated population structure from the full data set (Full) and 10 subsets of the data (S1-S10) (K=4).

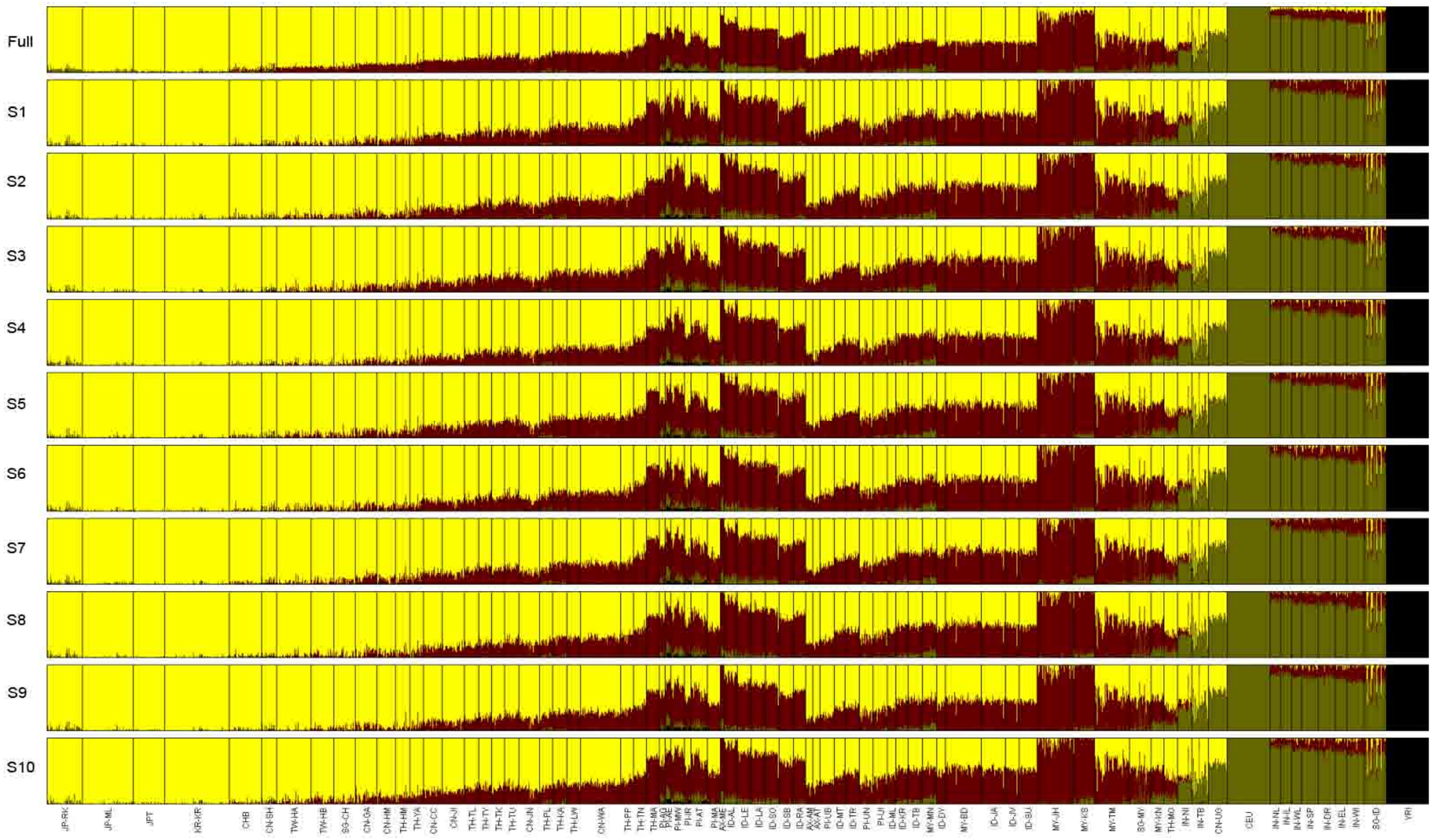

Figure S4 Estimated population structure from the full data set (Full) and 10 subsets of the data (S1-S10) (K=5).

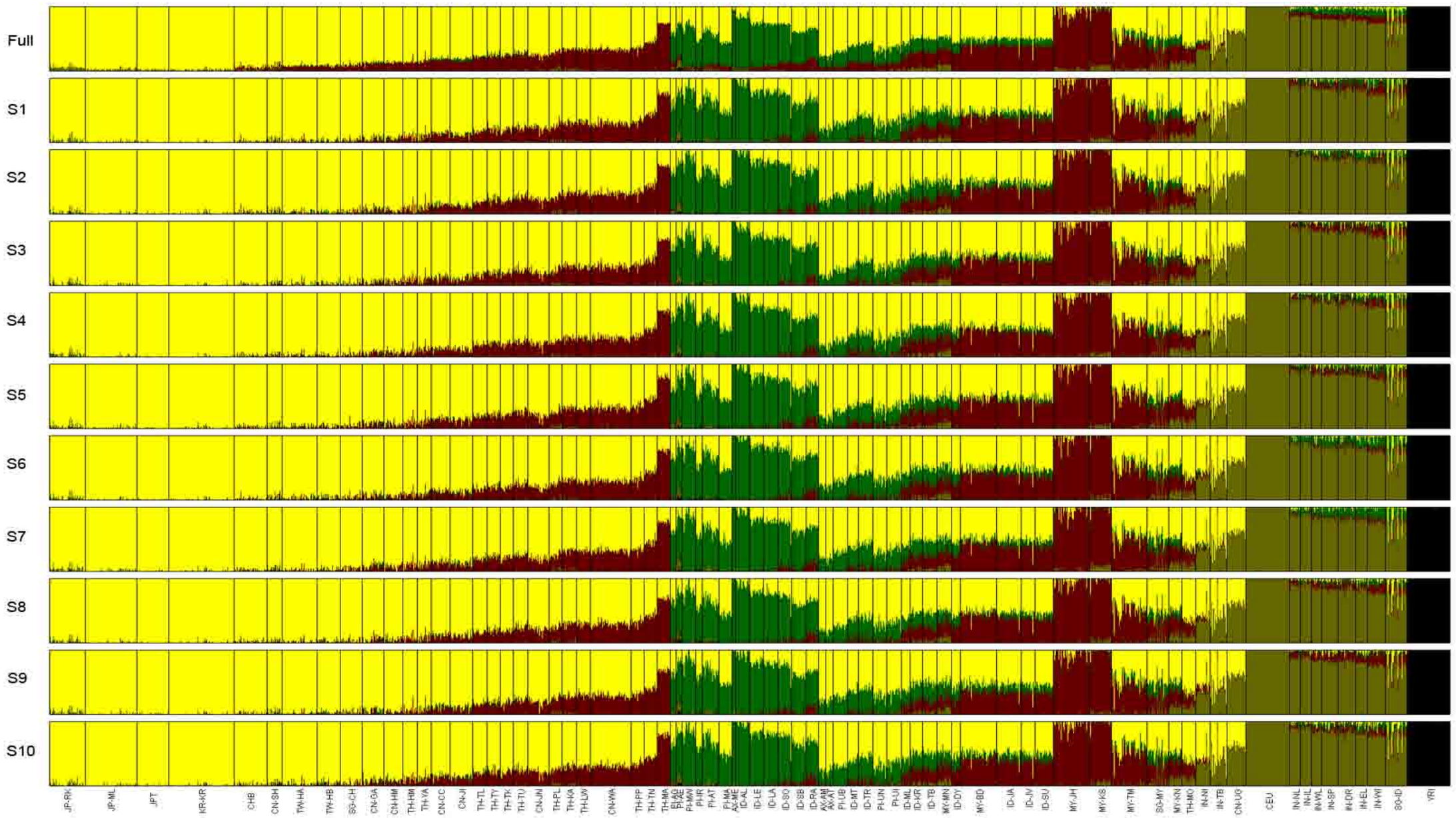

Figure S5 Estimated population structure from the full data set (Full) and 10 subsets of the data (S1-S10) (K=6).

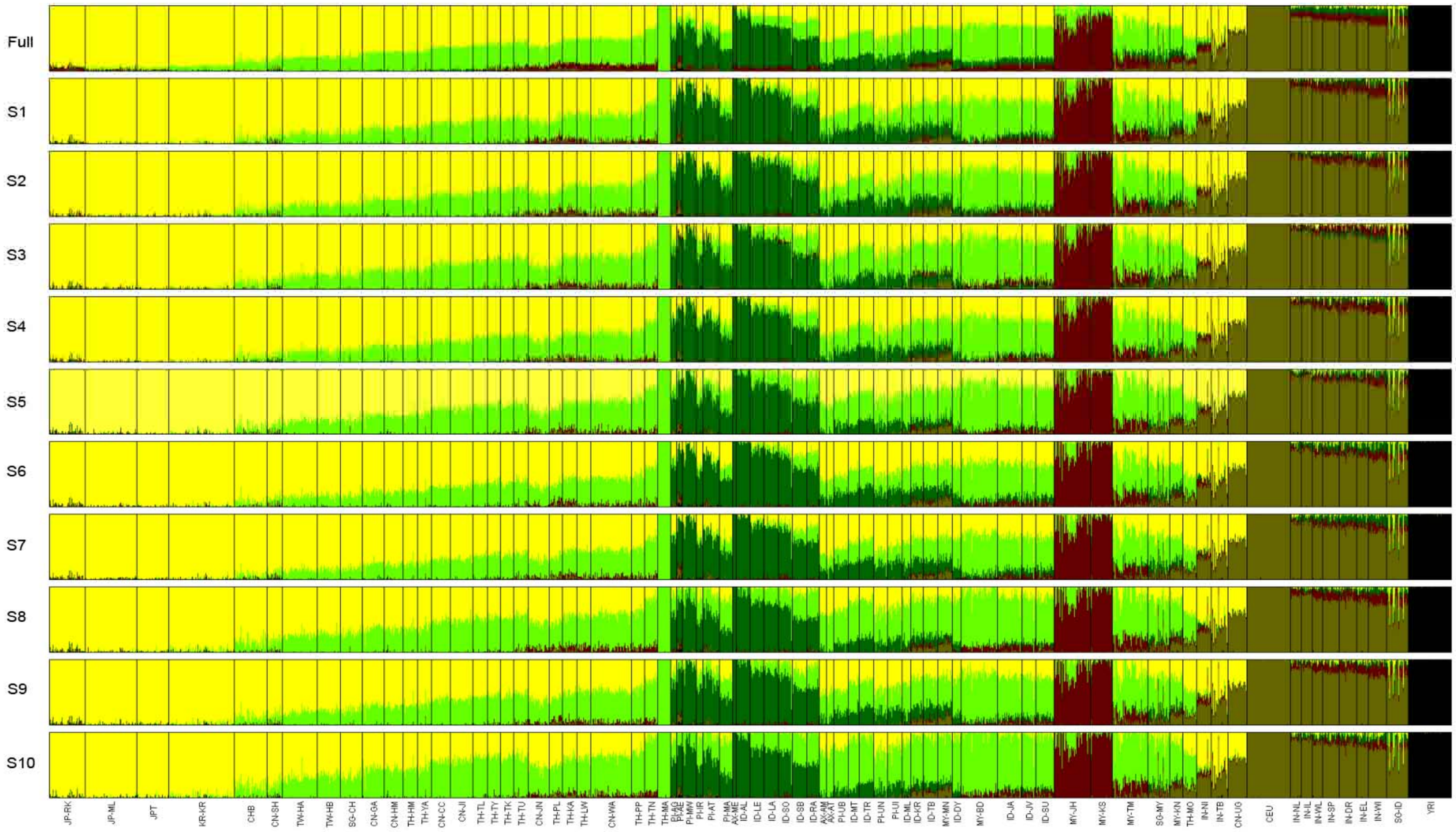

Figure S6 Estimated population structure from the full data set (Full) and 10 subsets of the data (S1-S10) (K=7).

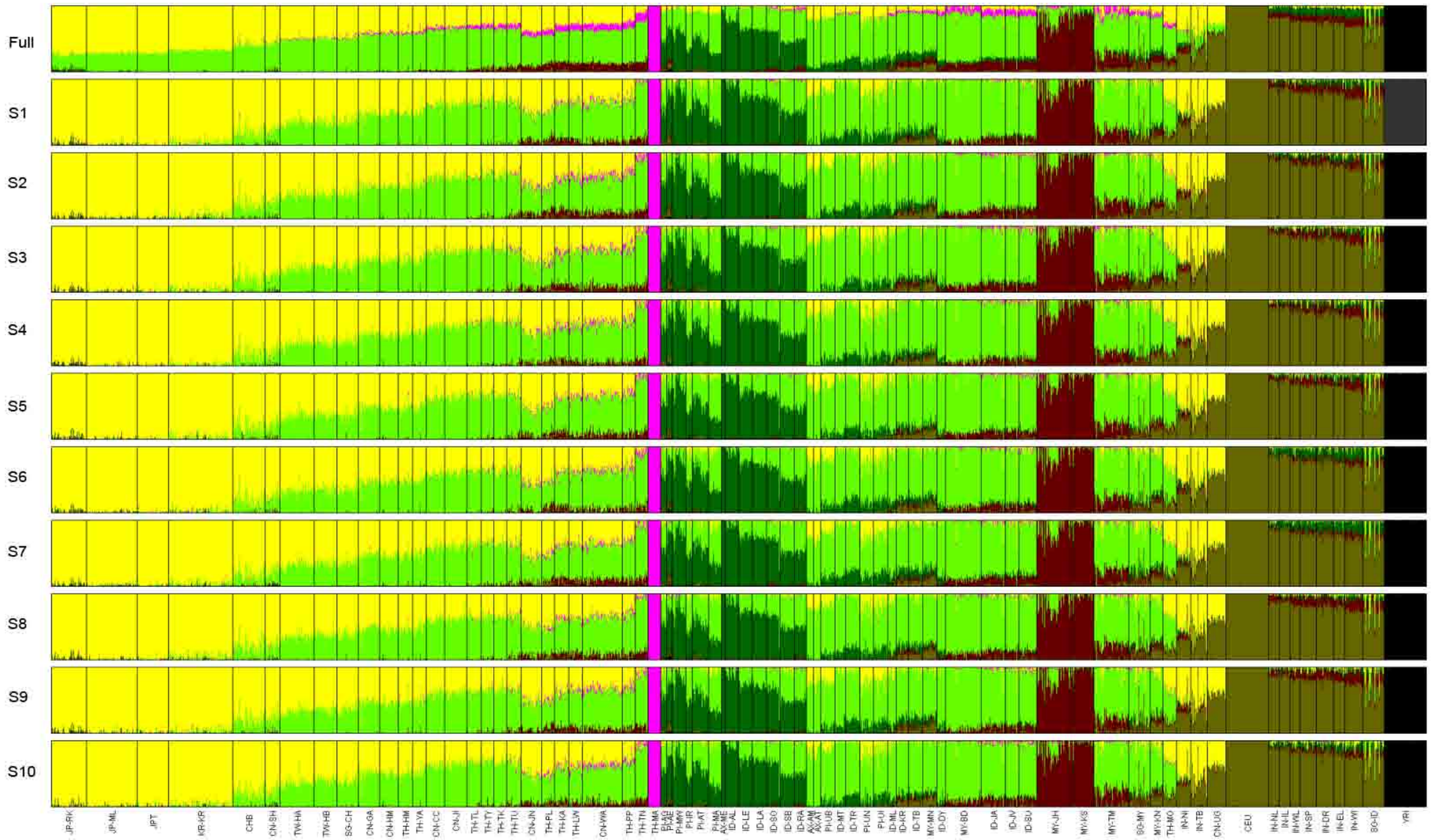

Figure S7 Estimated population structure from the full data set (Full) and 10 subsets of the data (S1-S10) (K=8).

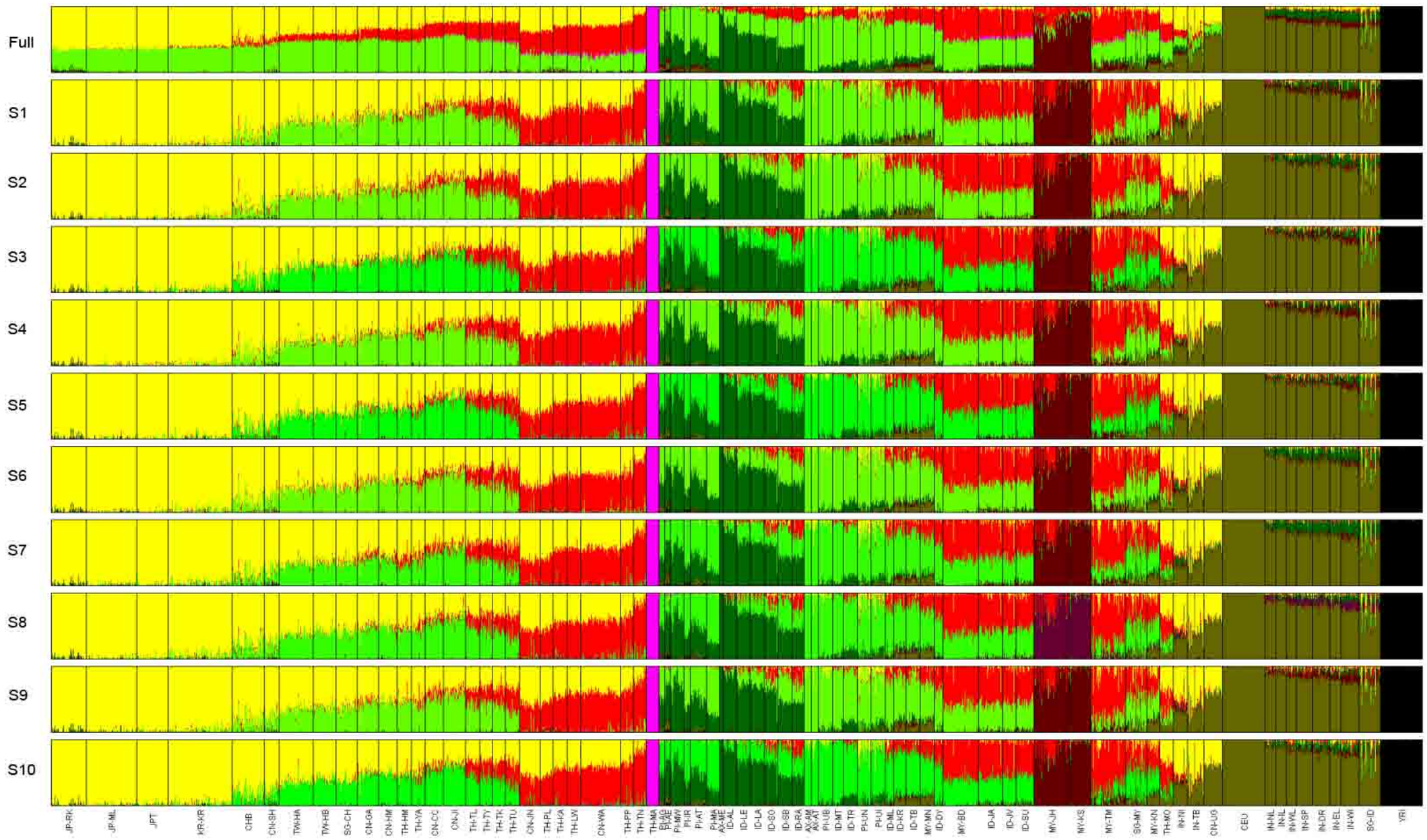

Figure S8 Estimated population structure from the full data set (Full) and 10 subsets of the data (S1-S10) (K=9).

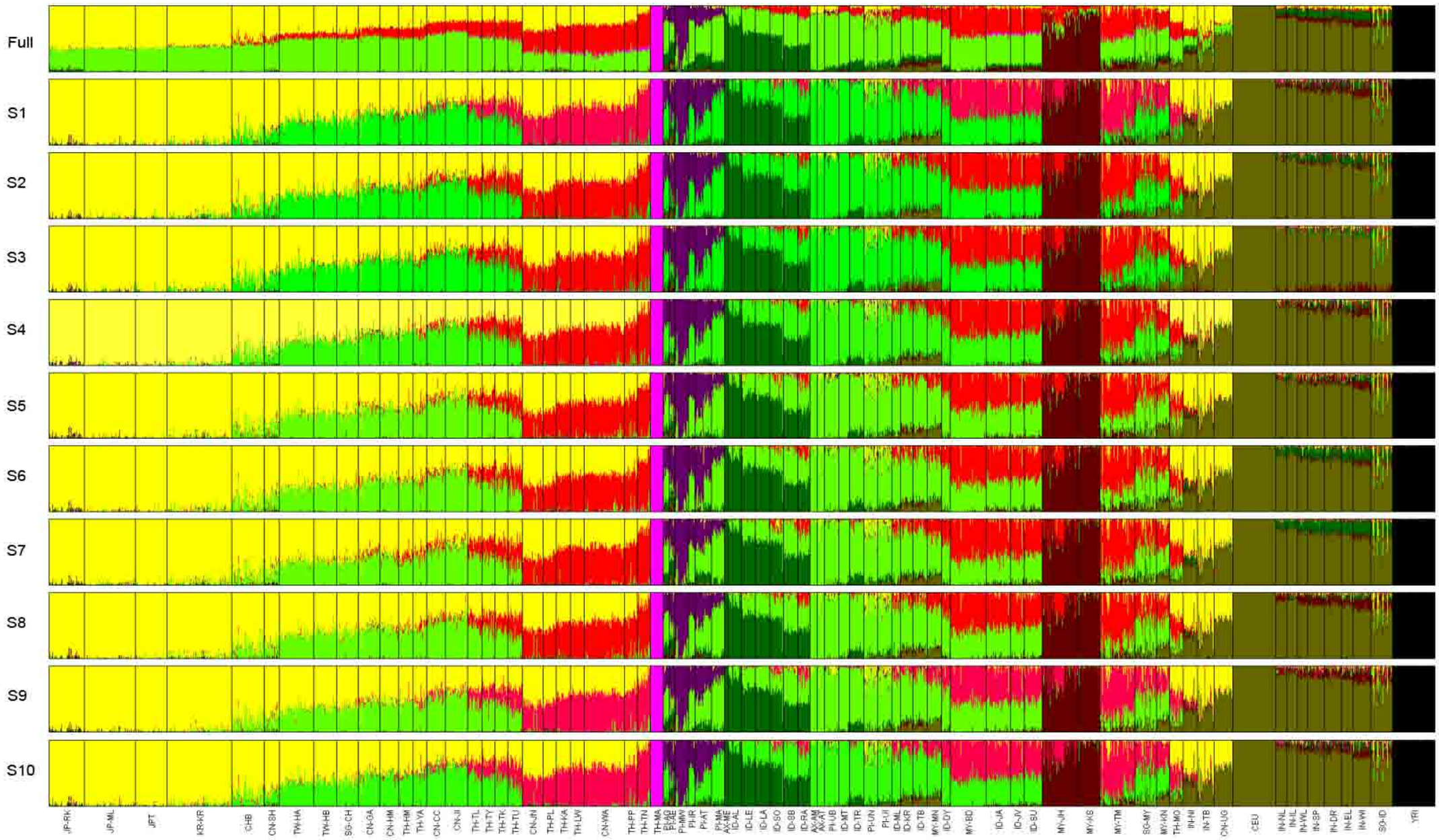

Figure S9 Estimated population structure from the full data set (Full) and 10 subsets of the data (S1-S10) (K=10).

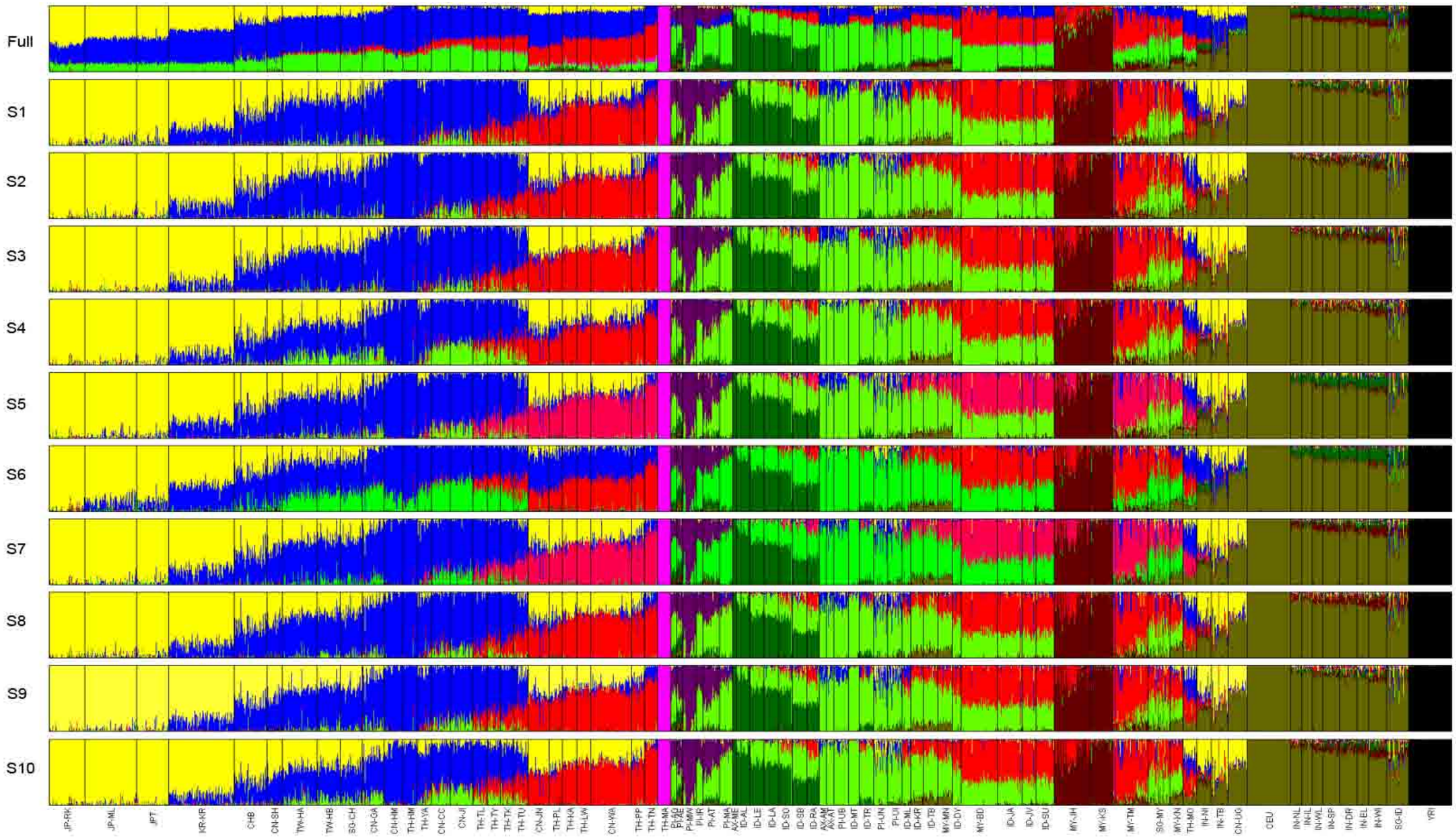

Figure S10 Estimated population structure from the full data set (Full) and 10 subsets of the data (S1-S10) (K=11).

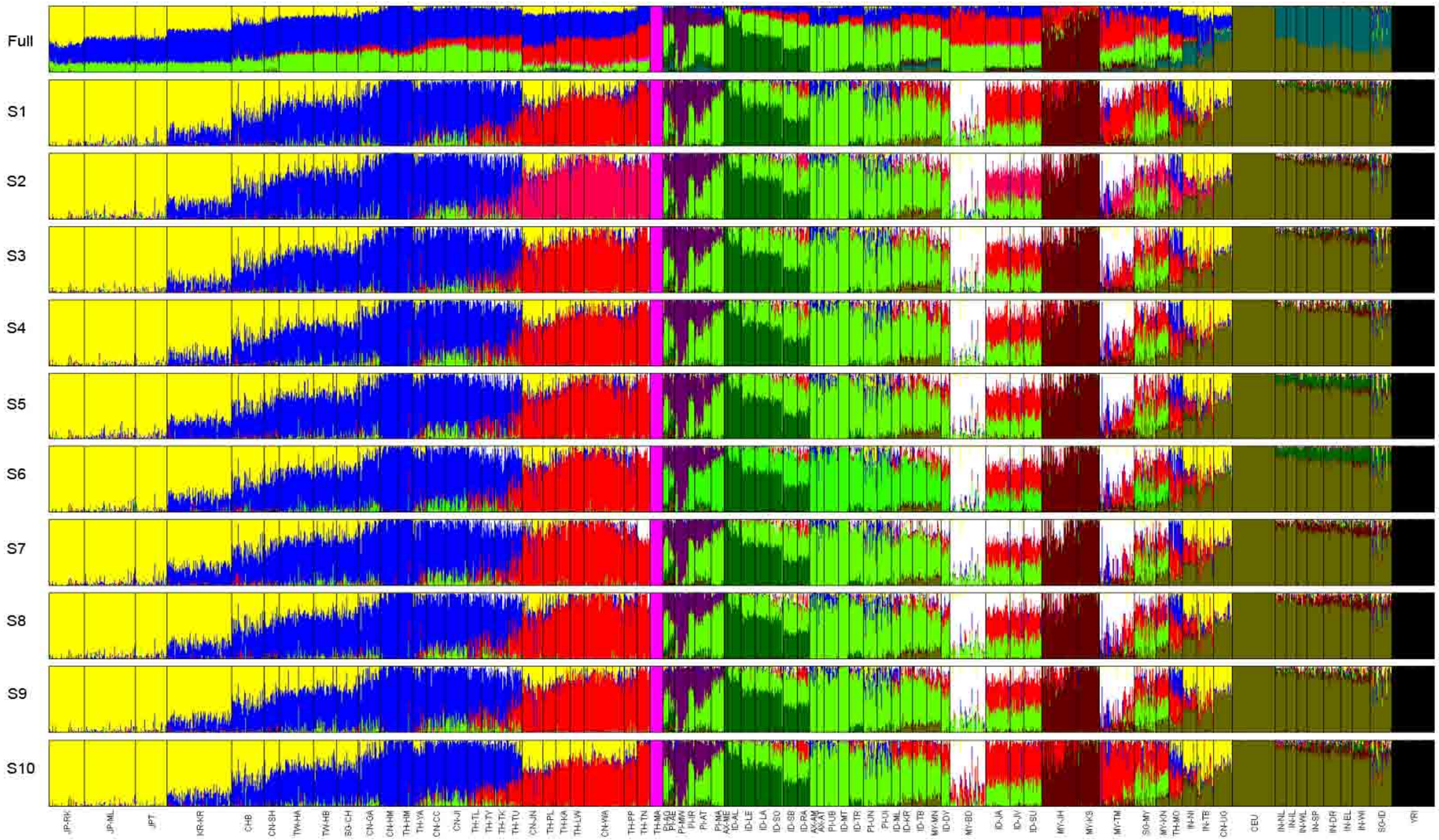

Figure S11 Estimated population structure from the full data set (Full) and 10 subsets of the data (S1-S10) (K=12).

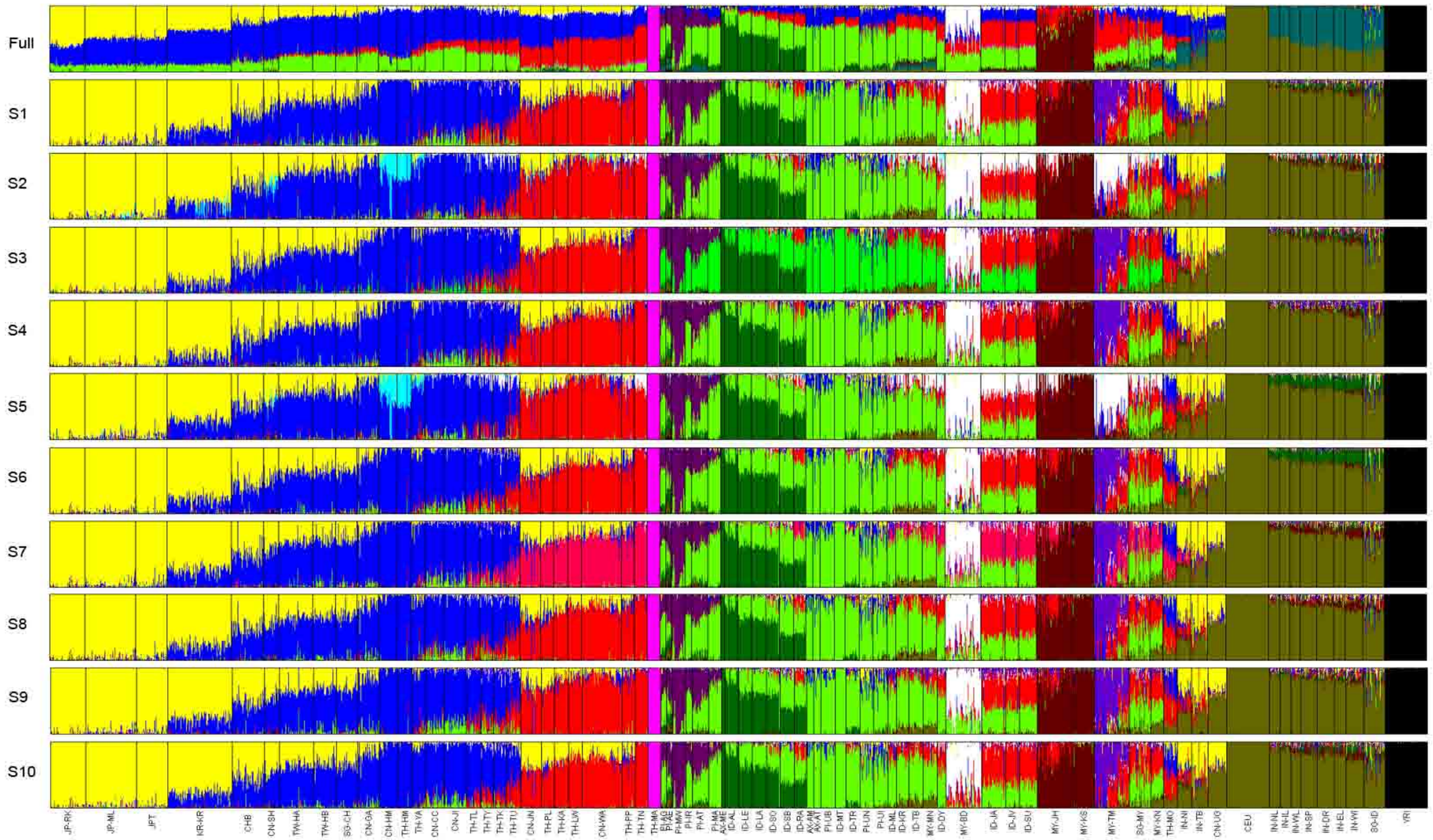

Figure S12 Estimated population structure from the full data set (Full) and 10 subsets of the data (S1-S10) (K=13).

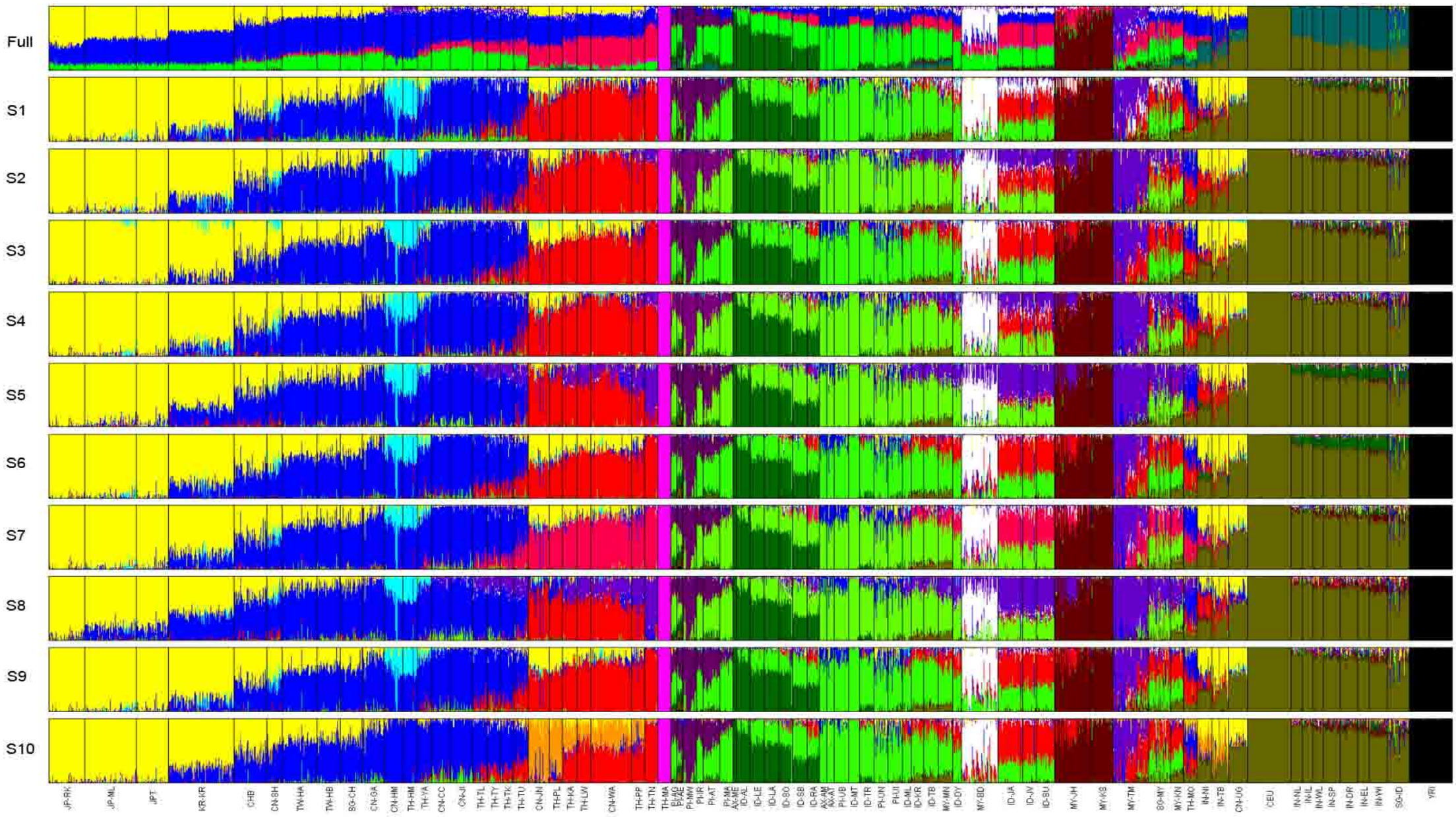

Figure S13 Estimated population structure from the full data set (Full) and 10 subsets of the data (S1-S10) (K=14).

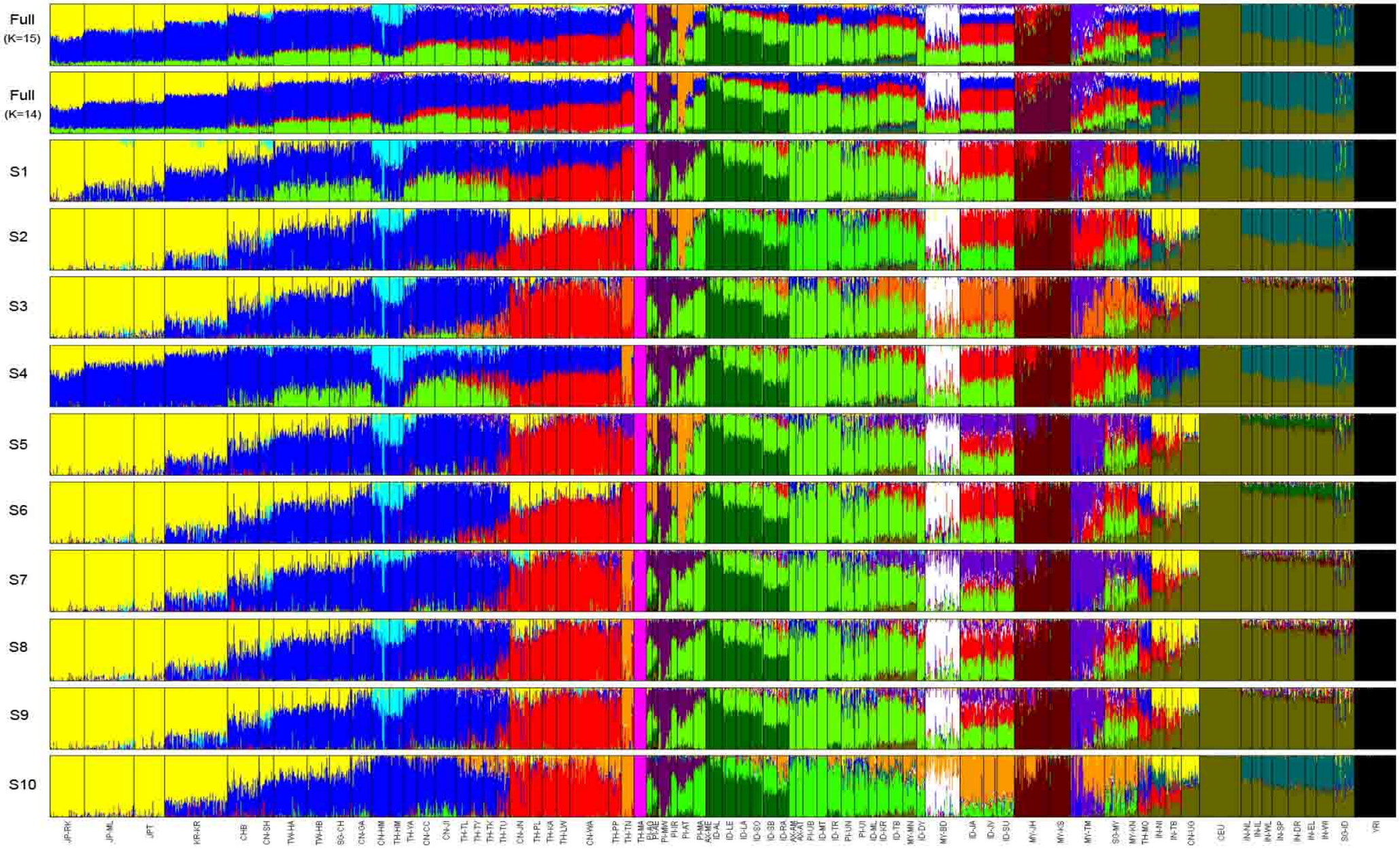

Figure S14 Estimated population structure from the full data set (Full) and 2 subsets of the data (S1-S2) (K=2).

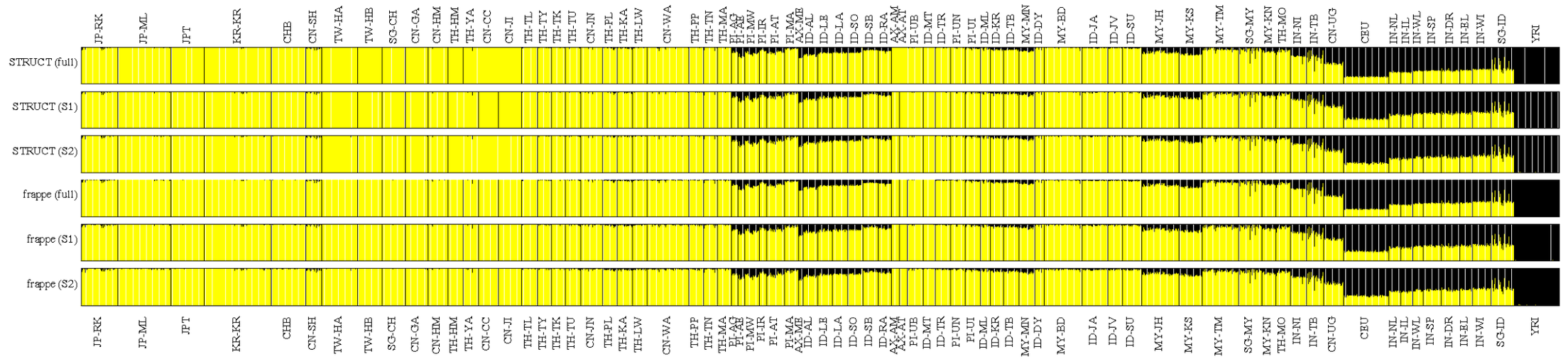

Figure S15 Estimated population structure from the full data set (Full) and 2 subsets of the data (S1-S2) (K=3).

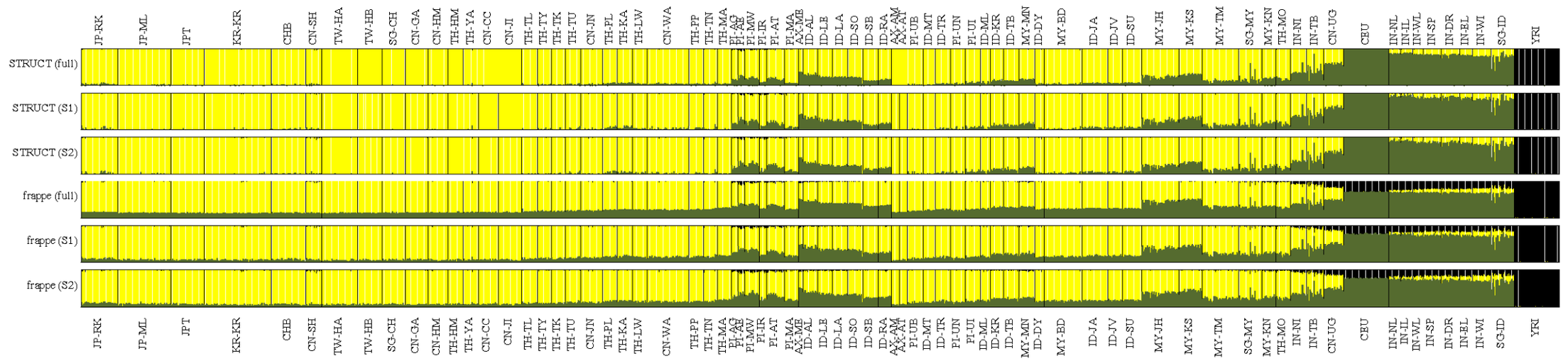

Figure S16 Estimated population structure from the full data set (Full) and 2 subsets of the data (S1-S2) (K=4).

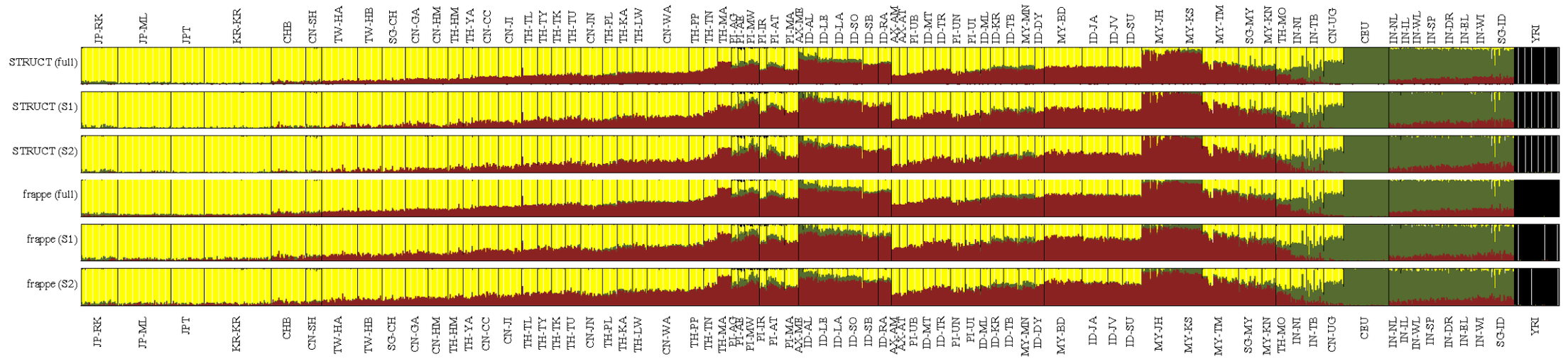

Figure S17 Estimated population structure from the full data set (Full) and 2 subsets of the data (S1-S2) (K=5).

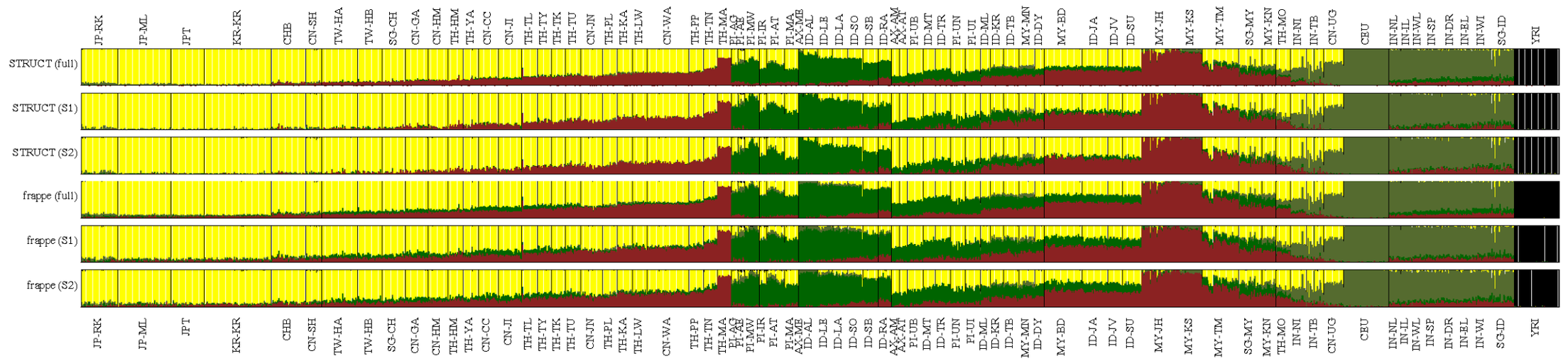

Figure S18 Estimated population structure from the full data set (Full) and 2 subsets of the data (S1-S2) (K=6).

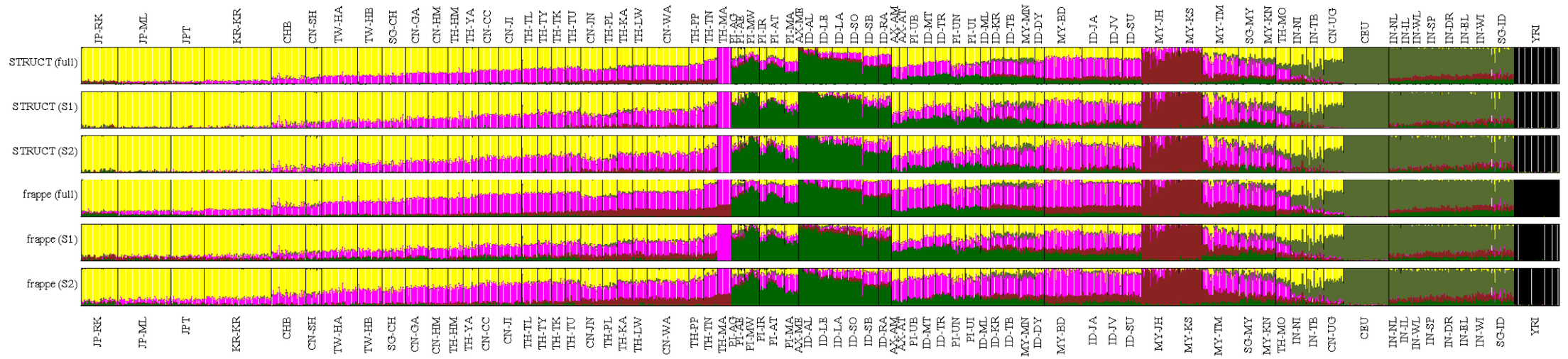

Figure S19 Estimated population structure from the full data set (Full) and 2 subsets of the data (S1-S2) (K=7).

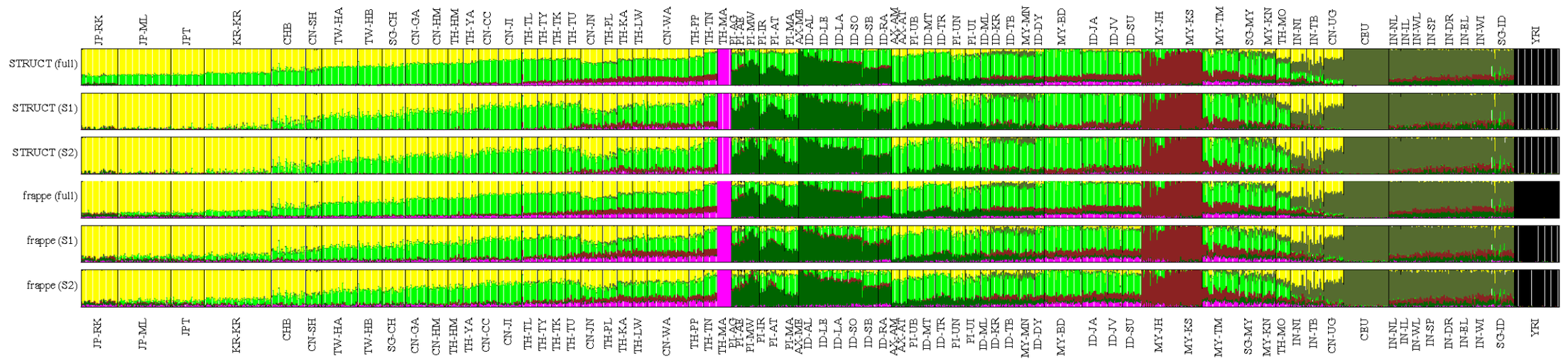

Figure S20 Estimated population structure from the full data set (Full) and 2 subsets of the data (S1-S2) (K=8).

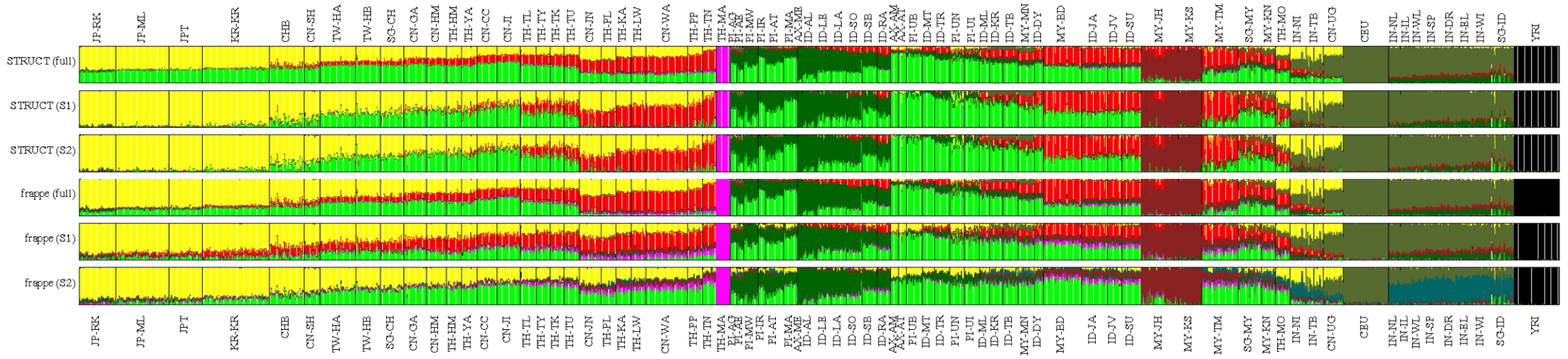

Figure S21 Estimated population structure from the full data set (Full) and 2 subsets of the data (S1-S2) (K=9).

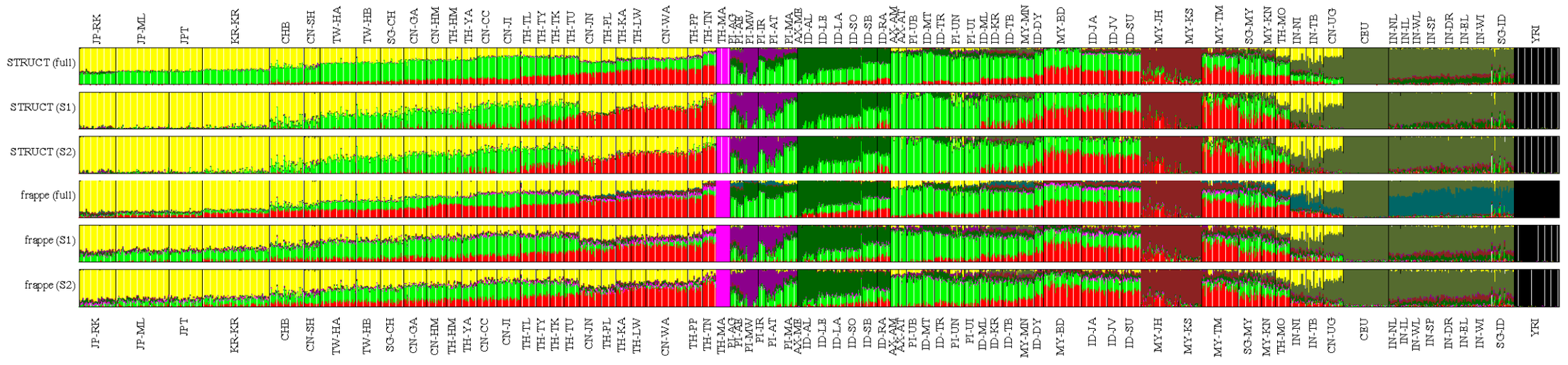

Figure S22 Estimated population structure from the full data set (Full) and 2 subsets of the data (S1-S2) (K=10).

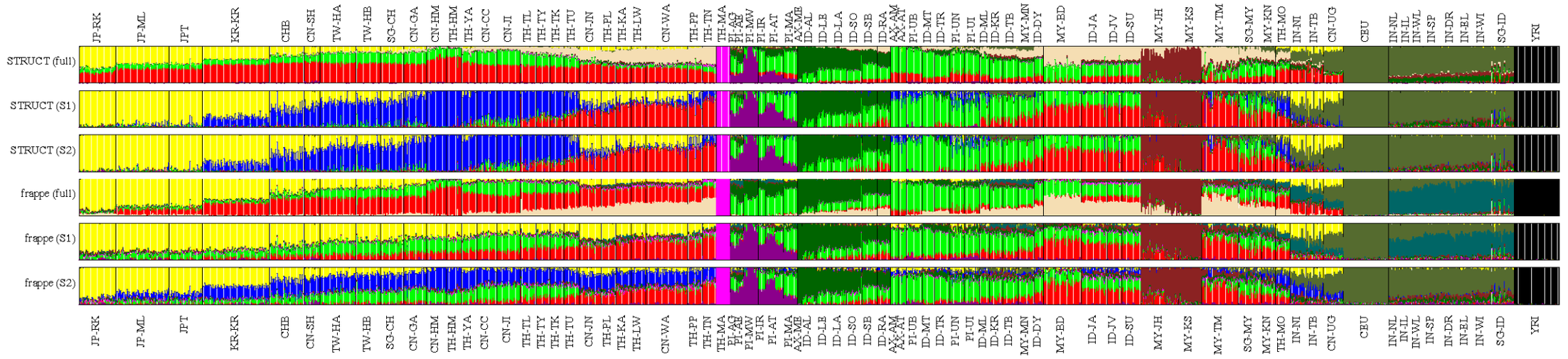

Figure S23 Estimated population structure from the full data set (Full) and 2 subsets of the data (S1-S2) (K=11).

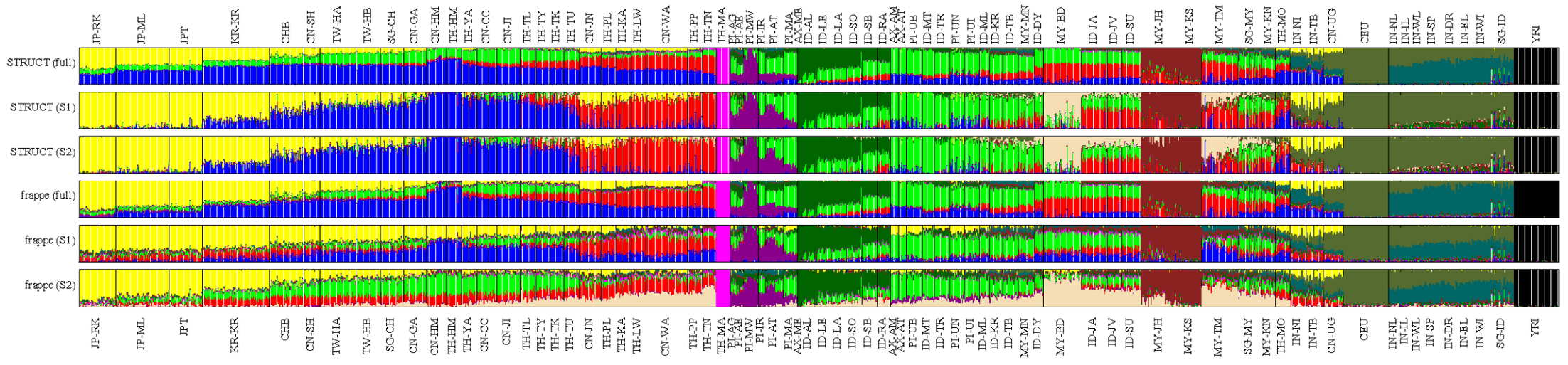

Figure S24 Estimated population structure from the full data set (Full) and 2 subsets of the data (S1-S2) (K=12).

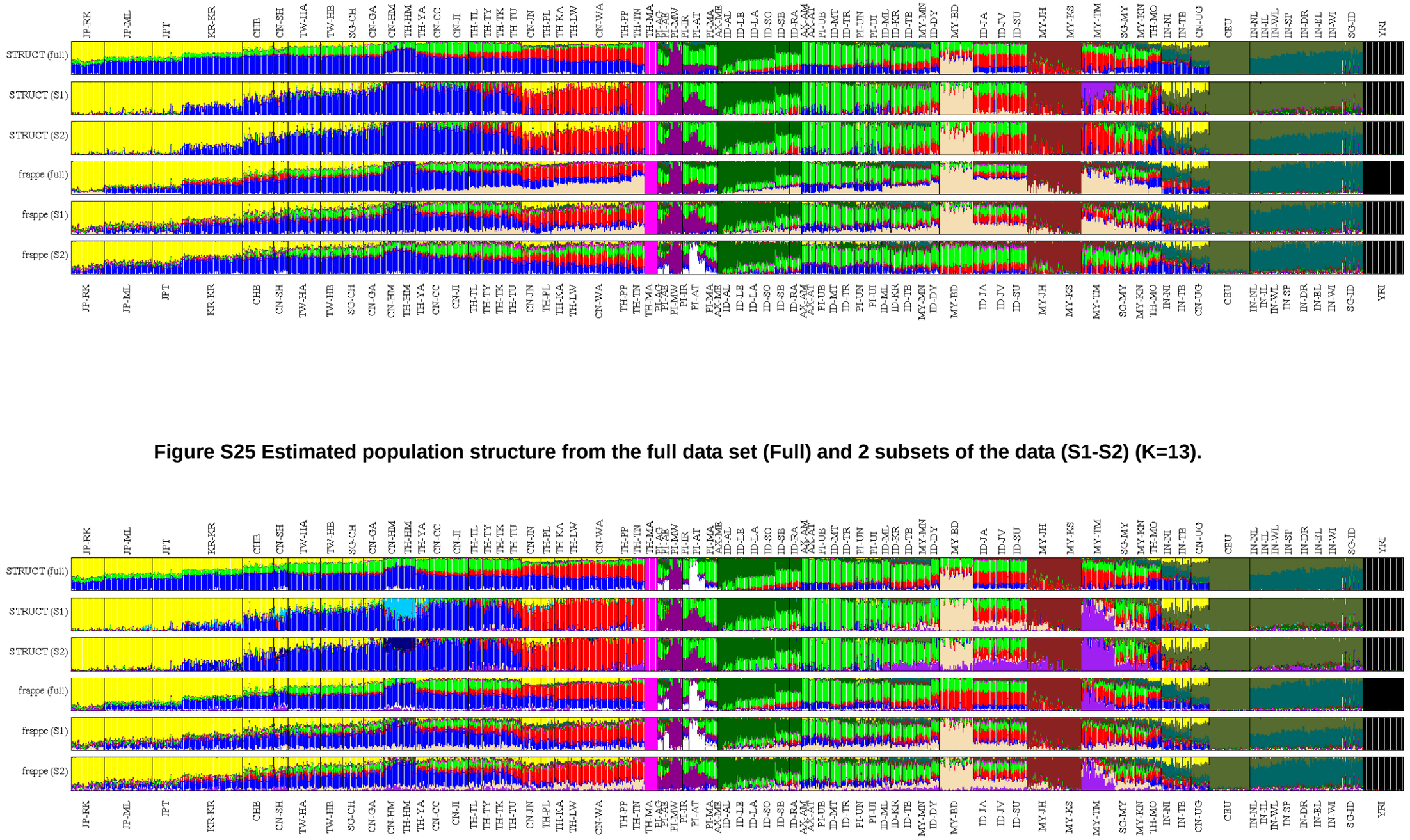

Figure S25 Estimated population structure from the full data set (Full) and 2 subsets of the data (S1-S2) (K=13).

Figure S26 Estimated population structure from the full data set (Full) and 2 subsets of the data (S1-S2) (K=14).

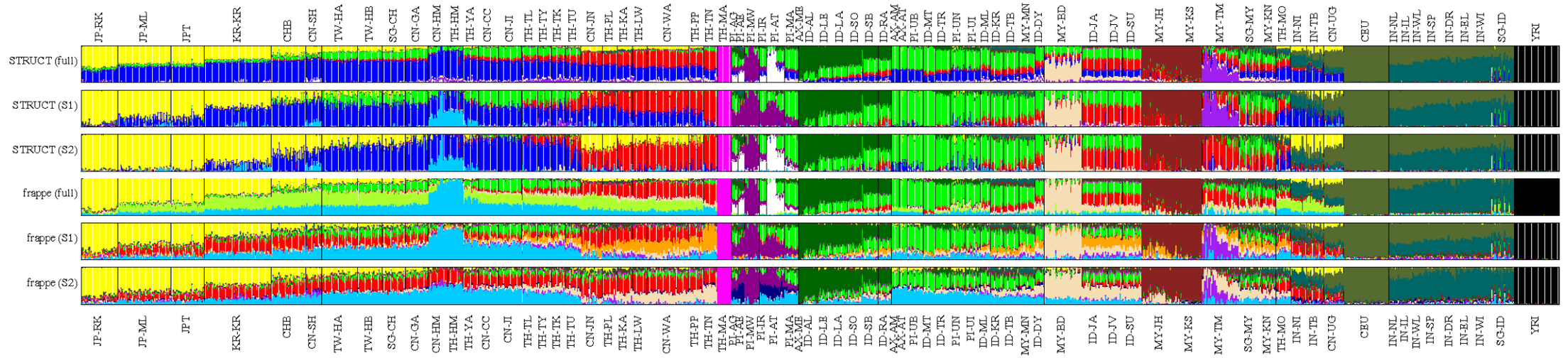

Figure S27 Neighbor-Joining tree of individuals based on the Allele Sharing Distance. The colors represent individuals of different language families as indicated in the legend.

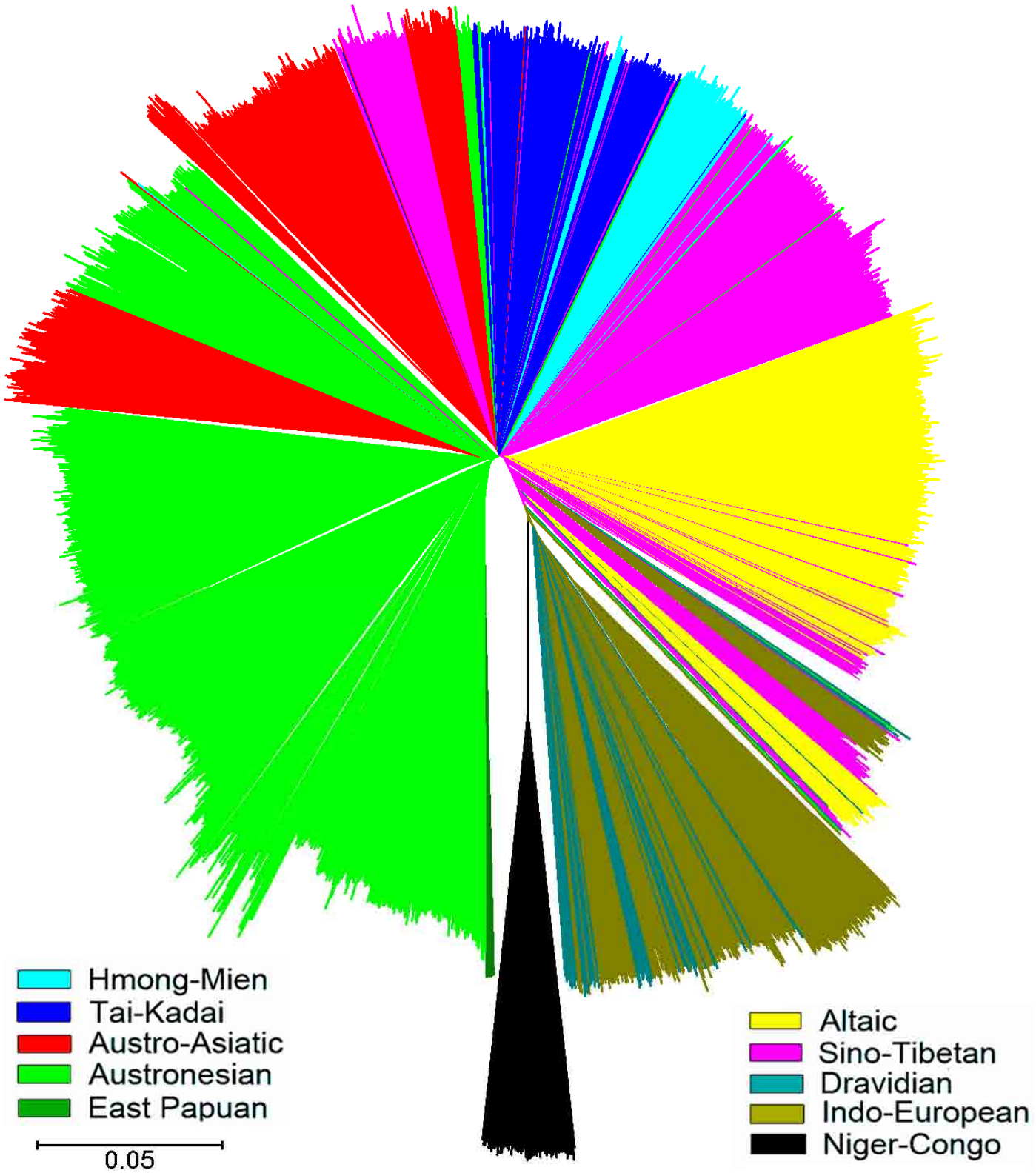

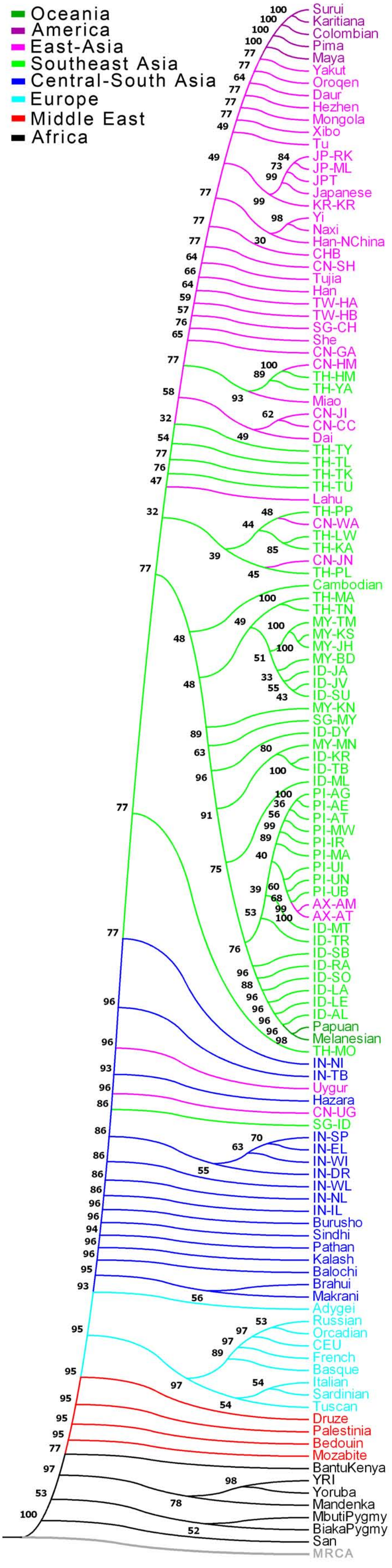
Oceania
America
East-Asia
Southeast Asia
Central-South Asia
Europe
Middle East
Africa
Surui
Karitiana
Colombian
Pima
Maya
Yakut
Oroqen
Daur
Hezhen
Mongola
Xibo
Tu
JP-RK
JP-ML
JPT
Japanese
KR-KR
Yi
Naxi
Han-NChina
CHB
CN-SH
Tujia
Han
TW-HA
TW-HB
SG-CH
She
CN-GA
CN-HM
TH-HM
TH-YA
Miao
CN-JI
CN-CC
Dai
TH-TY
TH-TL
TH-TK
TH-TU
Lahu
TH-PP
CN-WA
TH-LW
TH-KA
CN-JN
TH-PL
Cambodian
TH-MA
TH-TN
MY-TM
MY-KS
MY-JH
MY-BD
ID-JA
ID-JV
ID-SU
MY-KN
SG-MY
ID-DY
MY-MN
ID-KR
ID-TB
ID-ML
PI-AG
PI-AE
PI-AT
PI-MW
PI-IR
PI-MA
PI-UI
PI-UN
PI-UB
AX-AM
AX-AT
ID-MT
ID-TR
ID-SB
ID-RA
ID-SO
ID-LA
ID-LE
ID-AL
Papuan
Melanesian
TH-MO
IN-NI
IN-TB
Uygur
Hazara
CN-UG
SG-ID
IN-SP
IN-EL
IN-WI
IN-DR
IN-WL
IN-NL
IN-IL
Burusho
Sindhi
Pathan
Kalash
Balochi
Brahui
Makrani
Adygei
Russian
Orcadian
CEU
French
Basque
Italian
Sardinian
Tuscan
Druze
Palestinia
Bedouin
Mozabite
BantuKenya
YRI
Yoruba
Mandenka
MbutiPygmy
BiakaPygmy
San
MRCA

Figure S28 Maximum likelihood tree of 126 population samples. Bootstrap values based on 100 replicates are shown. Language families are indicated with colors as shown in the legend. All population IDs except the four HapMap samples (YRI, CEU, CHB and JPT) are denoted by four characters. The first two letters indicate the country where the samples were collected or (in the case of Affymetrix) genotyped according to the following convention: AX**: Affymetrix;** CN**: China;** ID**: Indonesia;** IN**: India;** JP**: Japan;** KR**: Korea;** MY**: Malaysia;** PI**: the Philippines;** SG**: Singapore;** TH**: Thailand;** TW**: Taiwan. The last two letters are unique ID's for the population. The rest population IDs are adopted from HGDP sample names.**

Figure S29 Hypothetical models of the peopling of Asia. Model 1 and Model 2 represent the “two waves” hypothesis, and Model 3 represents the “one wave” hypothesis. AF: African; NG: Negrito; AS: Asian; EU: European.

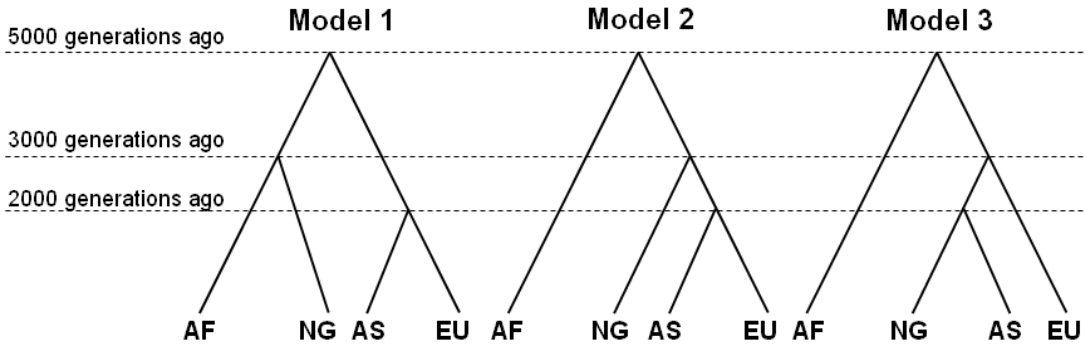

Figure S30 Simulated trees based on Model 1 and Model 2. M: gene flow proportion from AS to NG. Only those trees with either altered bootstrap values or topology are shown.

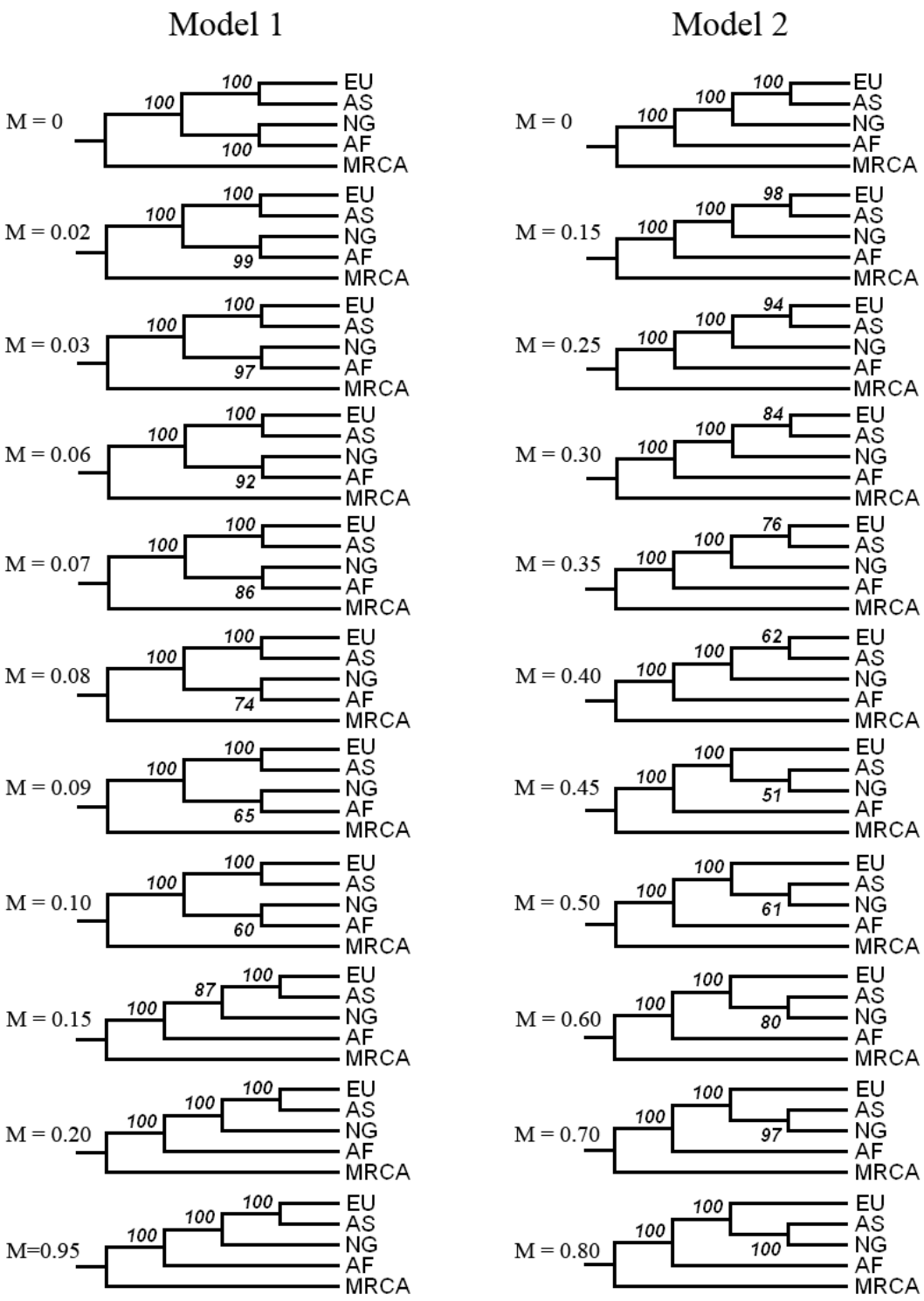

Figure S31 Geographical distribution of 71 PanAsia population samples and the 4 HapMap population samples.

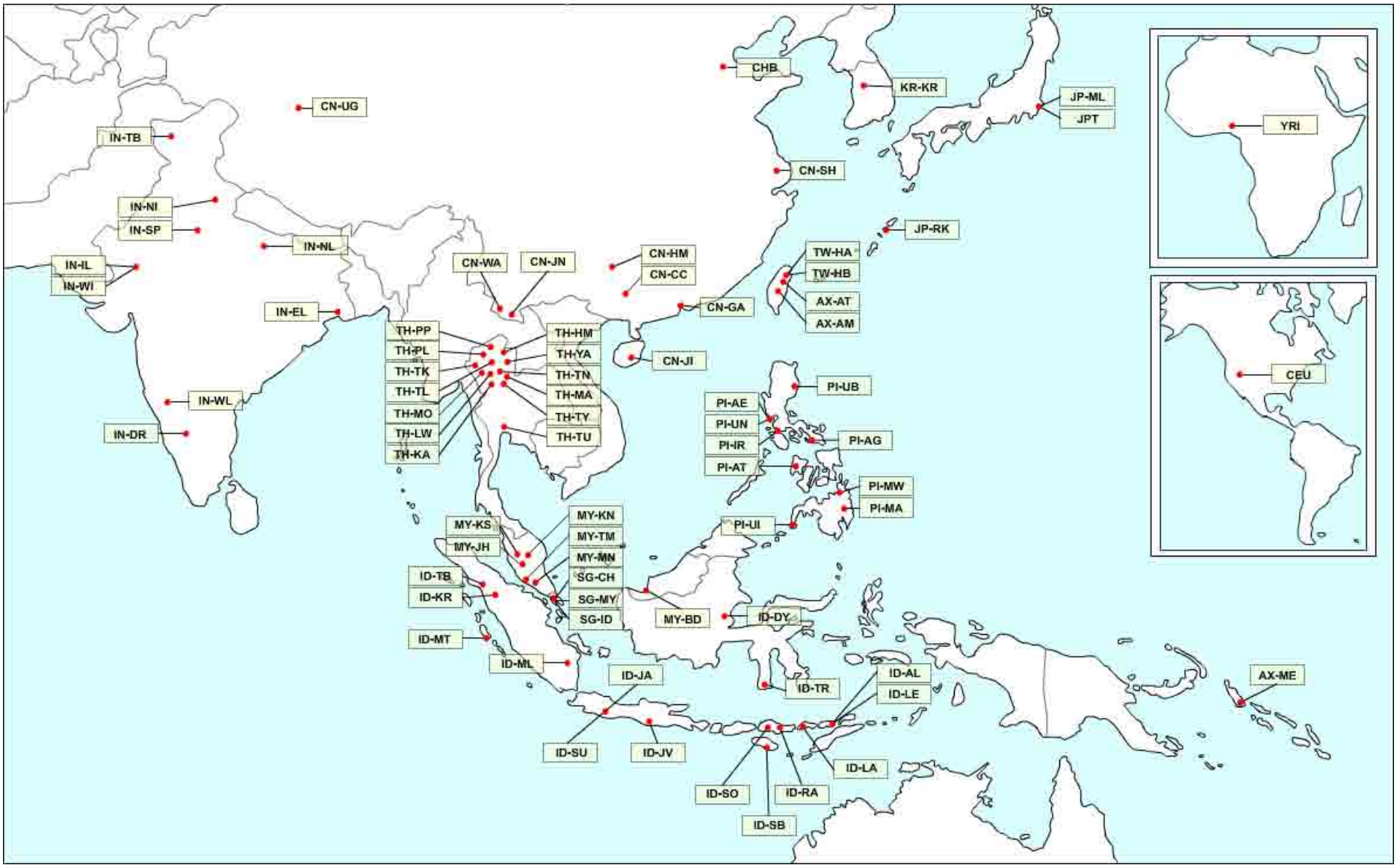

Figure S32 Distribution of sample sizes of different ethnic groupings or language families. The 75 populations represent 10 language families as shown in Figure 1. The Malaysian Negritos speak Austro-Asiatic languages and the Philippine Negritos speak Austronesian languages, but are shown separately. Sample sizes are shown in parentheses.

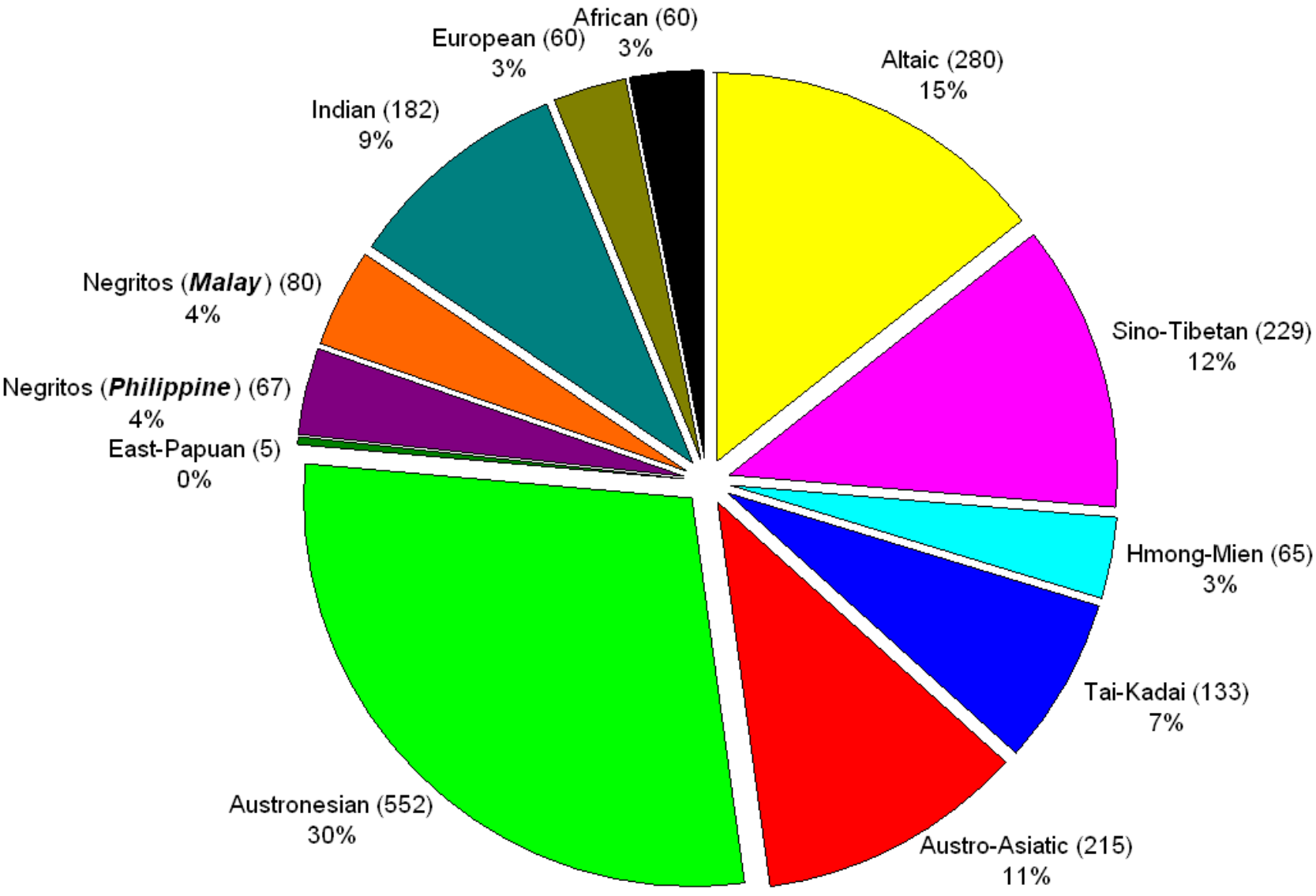

Figure S33 Comparison of pairwise FST between populations in full data set and sub-datasets. A: sub-dataset were obtained based on expected MAF spectrum in YRI; B: sub-dataset were obtained based on expected MAF spectrum in CEU; C: sub-dataset were obtained based on expected MAF spectrum in CHB; D: sub-dataset were obtained based on ENCODE MAF spectrum in YRI; E: sub-dataset were obtained based on ENCODE MAF spectrum in CEU; F: sub-dataset were obtained based on ENCODE MAF spectrum in CHB. The overall correlation coefficient for each comparison is as follows: 0.993 (A), 0.998 (B), 0.998 (C), 0.981 (D), 0.989 (E) and 0.992 (F).

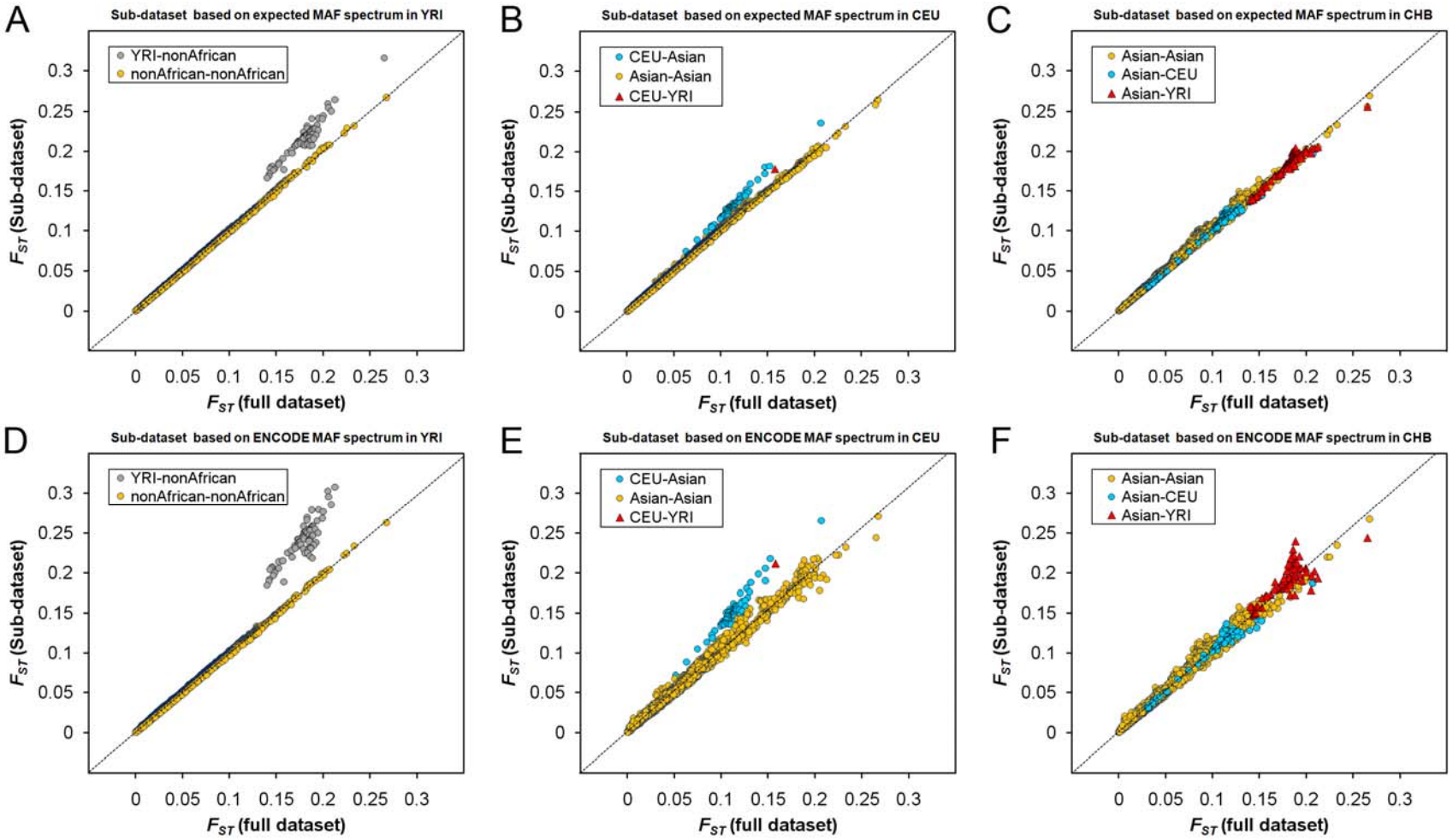

Figure S34 Maximum likelihood tree of 75 populations reconstructed from sub-datasets. The annotations of populations are the same as that in Figure 1. Branches with bootstrap values less than 50% were condensed. A: 100 sub-datasets of which SNPs were selected based on their expected allele frequency distribution in YRI. B: 100 sub-datasets of which SNPs were selected based on their expected allele frequency distribution in CEU. C: 100 sub-datasets of which SNPs were selected based on their expected allele frequency distribution in CHB.

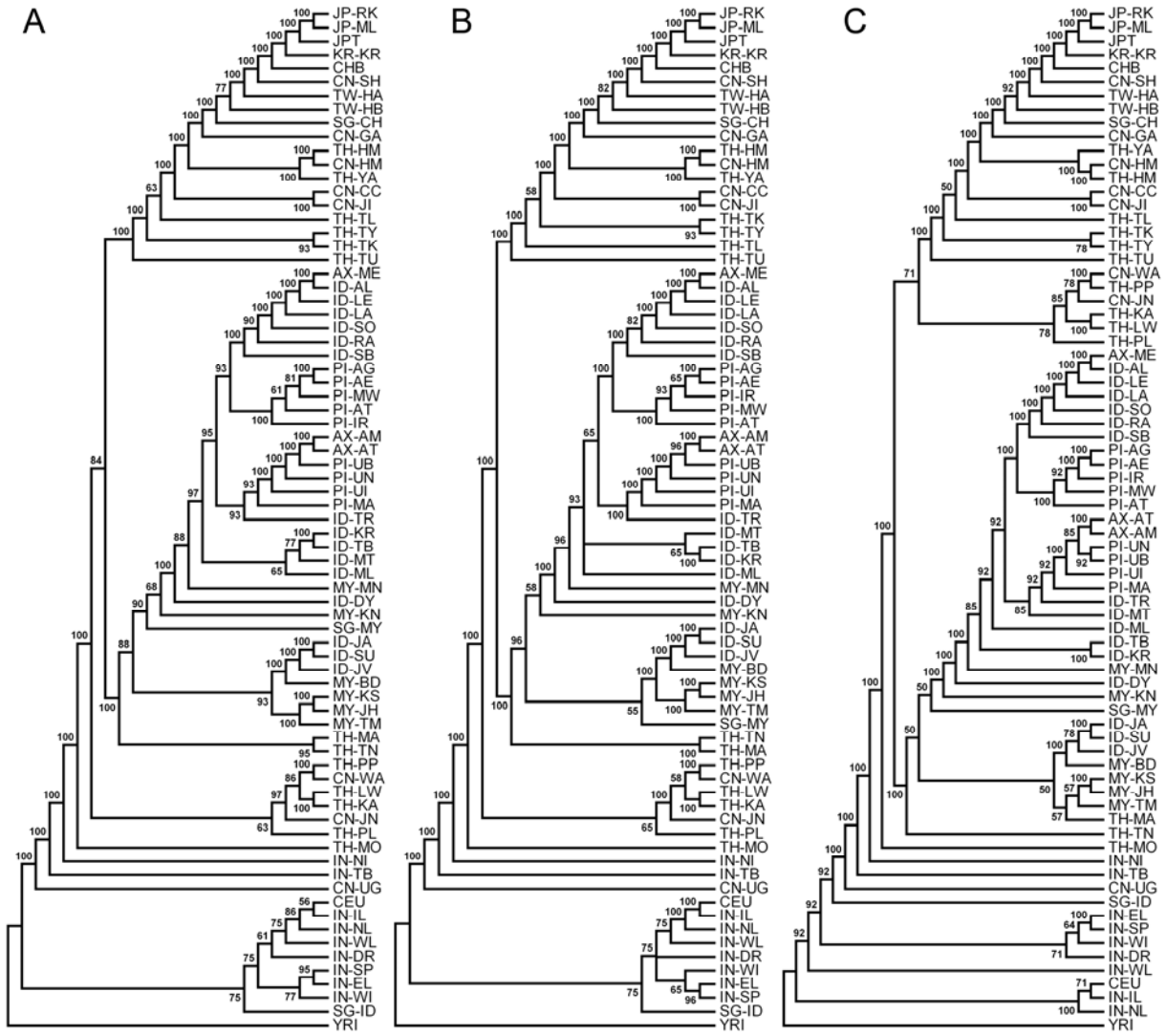

Figure S35 Maximum likelihood tree of 75 populations reconstructed from sub-datasets. The annotations of populations are the same as that in Figure 1. Branches with bootstrap values less than 50% were condensed. A: 100 sub-datasets of which SNPs were selected based on YRI allele frequency distribution in ENCODE regions. B: 100 sub-datasets of which SNPs were selected based on CEU allele frequency distribution in ENCODE regions. C: 100 sub-datasets of which SNPs were selected based on CHB allele frequency distribution in ENCODE regions.

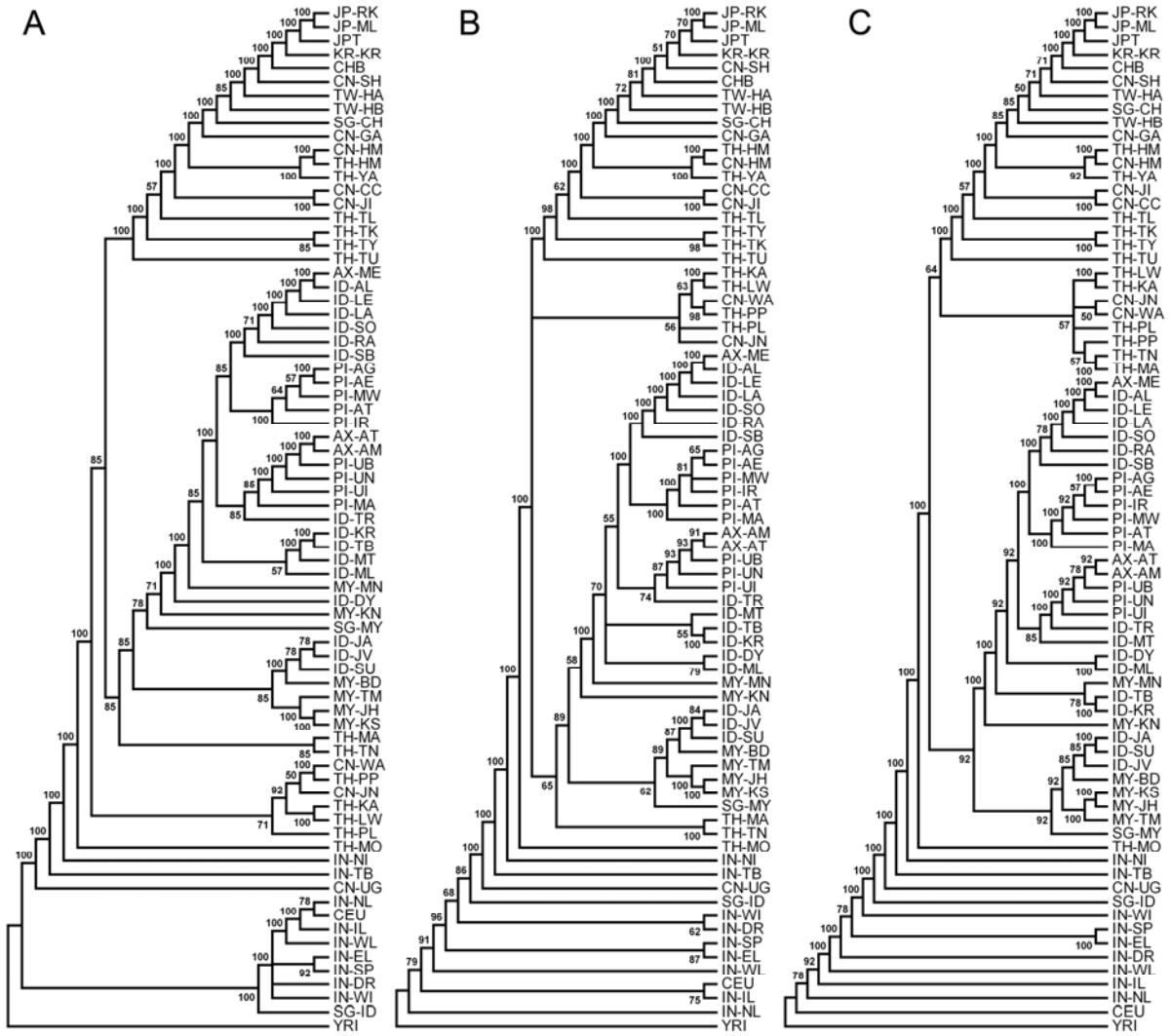

Figure S36 Maximum likelihood tree of 75 populations reconstructed from sub-datasets. The annotations of populations are the same as that in Figure 1. Branches with bootstrap values less than 50% were condensed. A: 100 sub-datasets of which SNPs were selected based on their expected allele frequency distribution in Malay Negritos (MY-NG). B: 100 sub-datasets of which SNPs were selected based on their expected allele frequency distribution in Philippine Negritos (PI-NG).

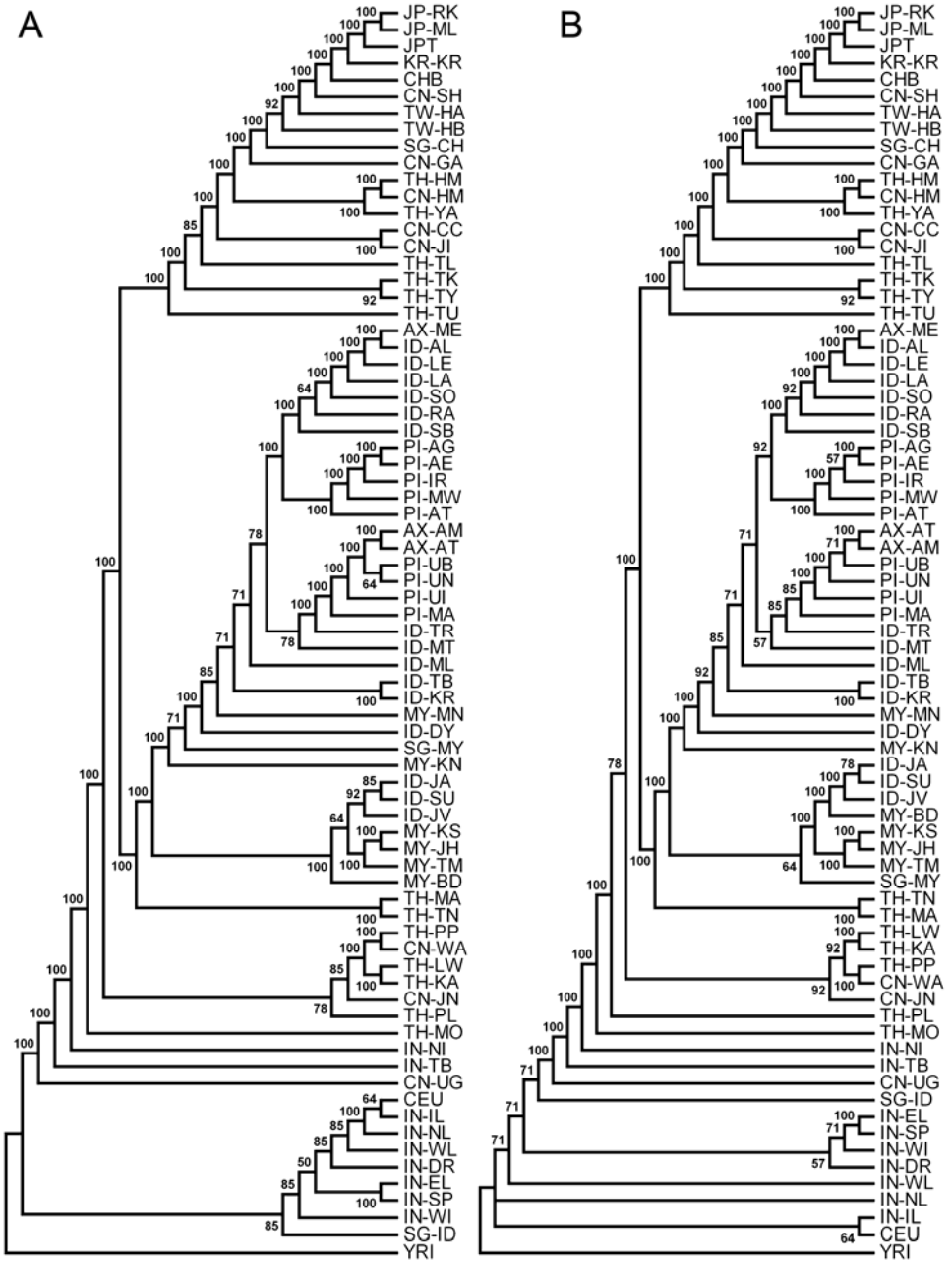

Figure S37 Haplotype diversity versus latitudes. Haplotypes were estimated from combined data and dieversity was measured by herterozygosity of haplotypes. ① Indonesian; ② Malay; ③ Philippine; ④ Thai; ⑤ South Chinese minorities; ⑥ Southern Han Chinese; ⑦ Japanese & Korean; ⑧ Northern Han Chinese; ⑨ Northern Chinese Minorities; ⑩ Yakut.

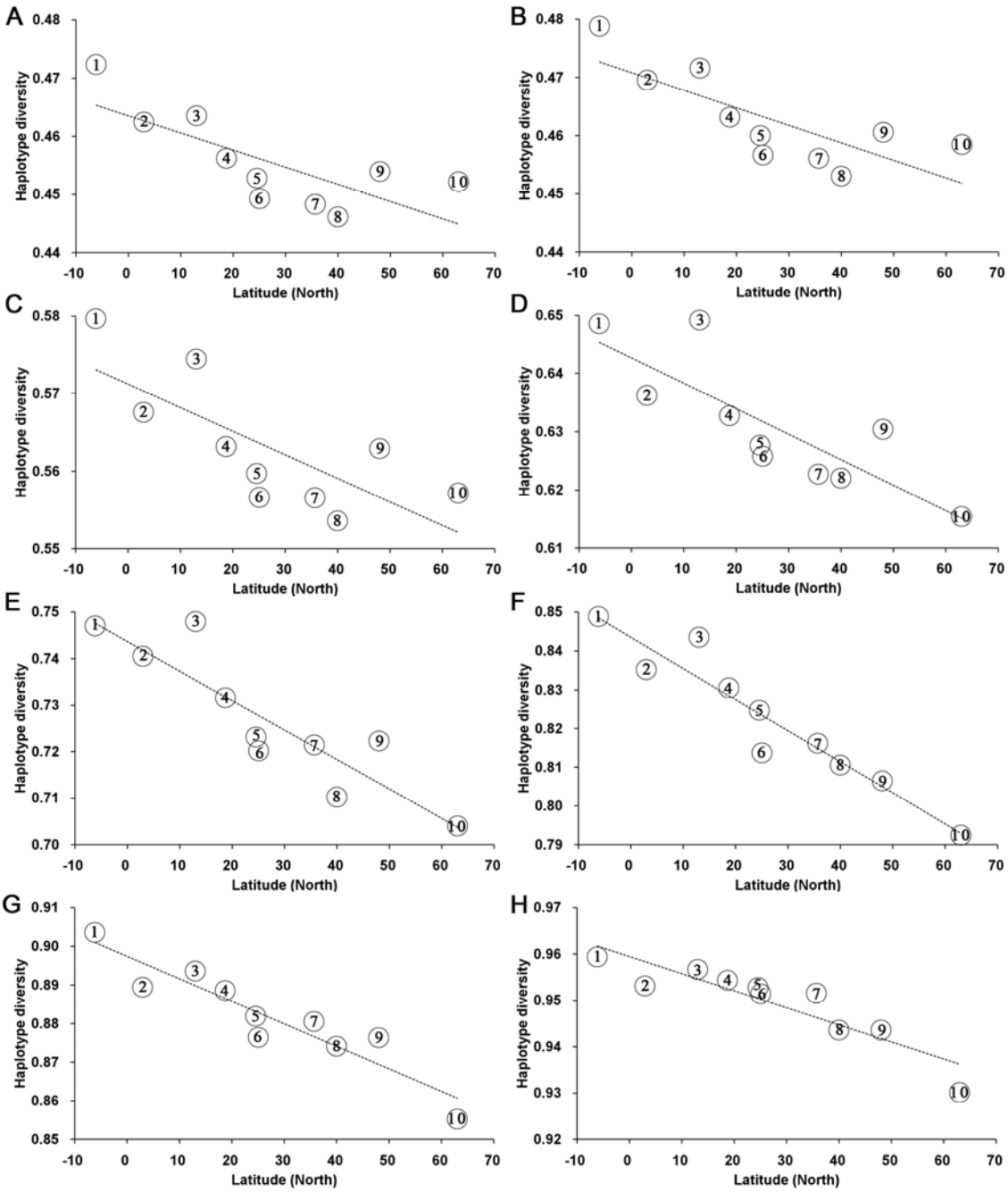

Figure S38 Group specific haplotype sharing analysis (PanAsia data). Haplotypes were estimated from PanAsia data. JP: Japanese; KR: Korean; HAN: Han Chinese; S-CM: Southern Chinese minorities; EA: East Asian.

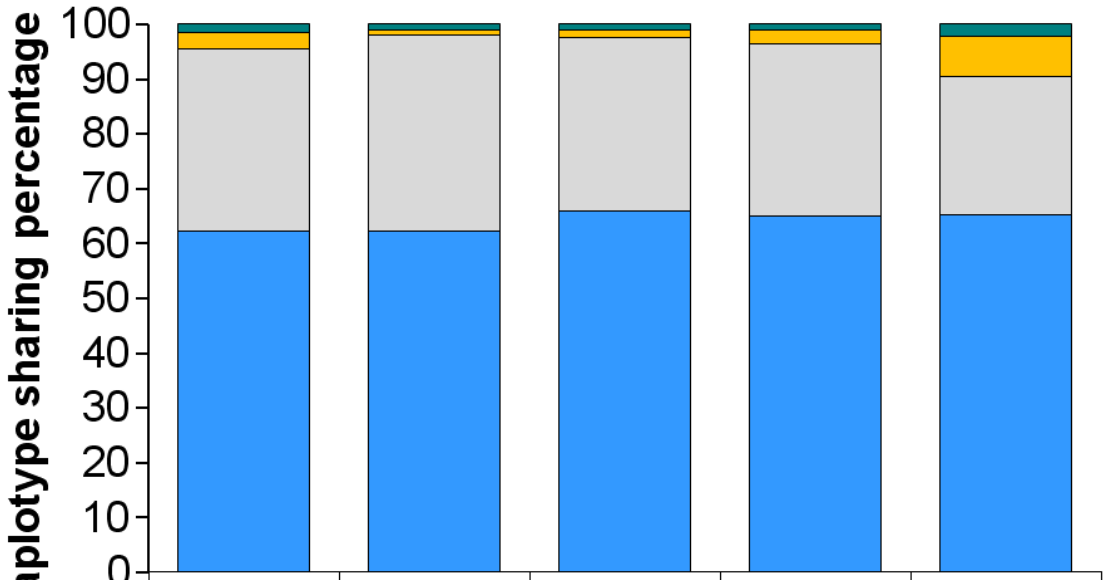

	JP	KR	HAN	S-CM	EA
HSa	1.5	1.1	1.2	1.1	2.2
HSb	3.1	0.9	1.4	2.5	7.3
HSc	33.1	35.6	31.5	31.5	25.4
HSd	62.0	61.8	65.7	64.7	65.0